GEOLOGICAL ASSOCIATION OF CANADA
ASSOCIATION GÉOLOGIQUE DU CANADA

Mineralogical Association of Canada
Association minéralogique du Canada

The Anvil District

Field trip leaders:
Lee Pigage and Dustin Rainey

May 30-31, 2016

Margins Through Time
Whitehorse, YT
GAC®-MAC 2016

INTRODUCTION

The Anvil Pb-Zn-Ag district is located in central Yukon immediately north of the Town of Faro, 200 km northeast of Whitehorse (Fig. 1). Five known stratiform deposits of the massive pyritic sulphide deposit type (Gustafson and Williams 1981) describe a curvilinear arc in plan view (Fig. 2). Pre-NI43-101 reserves for these deposits are listed in Table 1. The district contains an estimated total of 225 million tonnes of sulphide-bearing rock (Jennings and Jilson, 1986). Information on the stratiform pyritic sulphide deposits presented in this field trip is based largely on articles by Jennings and Jilson (1986) and Pigage (1990, 2004).

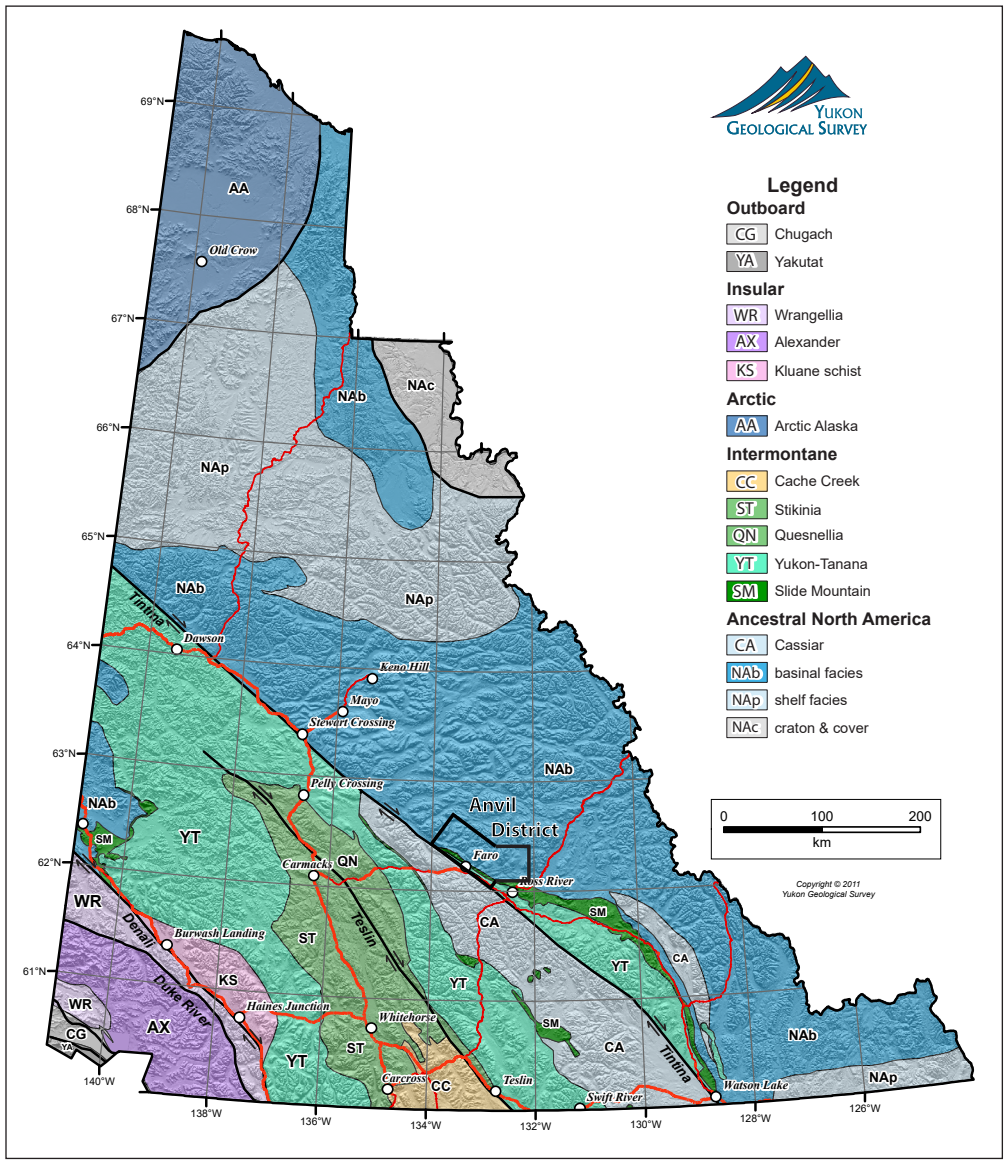

Figure 1. *Location of Anvil District within terrane map compilation for Yukon. Modified from Colpron and Nelson (2011); downloaded from* www.geology.gov.yk.ca/bedrock_terrane.html on February 1, *2016.*

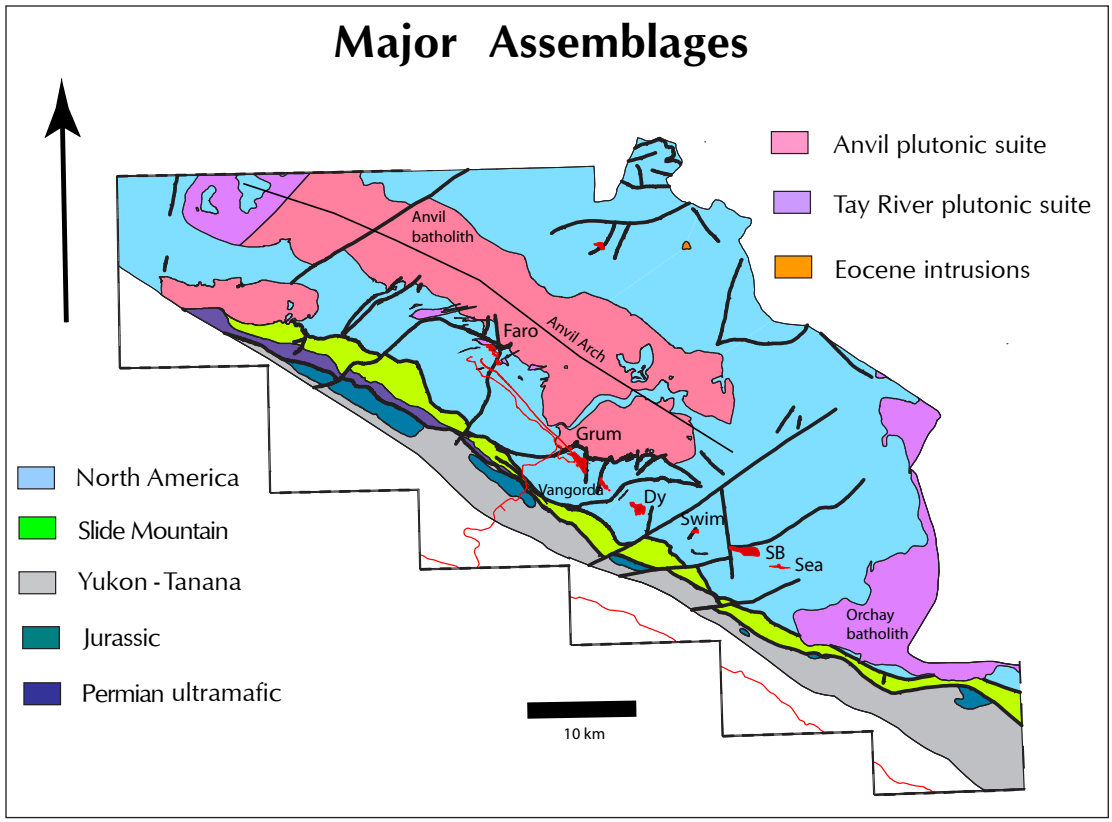

Figure 2. *Location of Anvil District stratiform sulphide deposits. Major rock assemblages within the District are indicated. Modified from Plate 2 of Pigage (2004).*

Table 1. Summary of tonnage and grade for Anvil district mineral deposits (Casselman, 2015).

Deposit	MINFILE	Tonnage x 10^6 tonnes	Category	Pb (%)	Zn (%)	Ag (g/mt)	Au (g/mt)
Faro	105K061	54.283	production	3.2	4.92	29.1	0.01
Grum	105K056	1.589	proven	3.56	5.34	58	0.83
		17.055	probable	2.6	4.34	44	0.74
Vangorda	105K055	4.55	production	2.48	3.48	27.3	
Dy / Grizzly	105K101	17.24	indicated	4.85	6.39	71.6	0.75
Swim	105K046	4.3	historic calculation	3.8	4.7	42	
SB	105K043		subeconomic				
Sea	105K042		subeconomic				
Total		99.017					

EXPLORATION HISTORY

In 1953 Al Kulan, Bert Law and Ted Chisholm staked mineral claims encompassing exposures of sulphides up to 10 feet high along the northwest bank of Vangorda Creek for a distance of over 100 feet. An extensive orange gossan extended downstream from the exposures. The gossan had previously been located by a prospecting group consisting of Jack Ladue, Robert Etzel, Joe Etzel, Peter Thompson, Art John, and Al Kulan, following up on Paul Sterriah stories of red-stained rocks in the creek (Gaffin, 1980). The mineral claims were immediately optioned by Prospectors Airways Company Limited. Prospectors Airways commenced drilling as a follow-up to extensive ground geochemical, geological and geophysical surveys which delineated a small zinc-lead-silver-barite massive sulphide deposit. The various ground surveys (Chisholm, 1957) were quickly adopted for other regional exploration programs throughout the area.

Four additional zinc-lead-silver-barite massive sulphide mineral deposits and two non-economic sulphide occurrences were discovered in the area between 1964 and 1976 (see Table 2). The discovery of the Faro deposit in 1964 resulted in the largest staking rush in Yukon to that date.

In 1979 Cyprus Anvil Mining Corporation purchased the Grum, Vangorda, and Swim deposits from Kerr Addison Mines Limited, consolidating all of the stratiform sulphide deposits under a single owner. Exploration for further stratiform deposits continued until 1998, when the current owner, Anvil Range Mining Corporation went into receivership.

More recently, exploration in the district has focussed on polymetallic, intrusion-related quartz veins and bulk tonnage targets. Yukon MINFILE occurrences also denote the presence of barite deposits and volcanic-hosted massive sulphide mineralization.

Table 2. *Discovery dates for mineral deposits and occurrences, Anvil district.*

Deposit	MINFILE	Discovery Date	Principal Discovery Method
Vangorda	105K055	1953	Conventional prospecting, confirmed by drilling in 1953
Sea	105K042	1964	Airborne magnetic/electromagnetic, ground gravity, geochemistry, confirmed by drilling in 1964
Swim	105K046	1964	Airborne magnetic/ground gravity, confirmed by drilling in 1965
SB	105K043	1964	Airborne magnetic, confirmed by drilling in 1965
Faro	105K061	1965	Airborne magnetic/ground electromagnetic, confirmed by drilling in 1965
Grum	105K056	1973	Gravity/airborne/magnetic/geology, confirmed by drilling in 1973
Dy / Grizzly	105K101	1976	Geology, confirmed by drilling in 1976

MINING HISTORY

Open pit mining of the Faro deposit at rates up to 10 000 tonnes per day began in 1969 as a joint venture between Dynasty Exploration and Cyprus Mines (initially called Anvil Mining Corporation and later Cyprus Anvil Mining Corporation). Zinc and lead concentrates were trucked to Whitehorse where they were transferred to the White Pass and Yukon Railway and transported to the port of Skagway, Alaska. Mining continued with some interruptions until 1982, when Cyprus Anvil Mining Corporation went into receivership.

The assets of Cyprus Anvil Mining Corporation were sold to Curragh Resources Inc. Curragh resumed open pit mining at a rate up to 13 500 tonnes per day in late 1986. Concentrates were trucked directly to Skagway using the South Klondike Highway. Grubbing and stripping of the Grum and Vangorda deposits for future open pit mining began in the late 1980s. Ore production from the Vangorda deposit began in 1990; ore was trucked 13 km to the Faro minesite for crushing and milling. All operations at the Faro, Vangorda and Grum mines ceased in 1993 with Curragh Resources going into receivership.

Anvil Range Mining Corporation acquired the assets of Curragh Resources in the Anvil district in 1994. Production from the Grum and Vangorda deposits began in 1995. The Vangorda deposit was mined out in 1996. Production at the Grum deposit continued until 1998. All mining stopped in early 1998 with Anvil Range Mining Corporation going into receivership.

In 2003 the Government of Yukon and the Government of Canada agreed to permanently close the fully mined Vangorda and Faro deposits and the partially mined Grum deposit. Consultation began on reclamation and closure plans. Remediation is being managed by the Assessment and Abandoned Mines Branch within the Energy, Mines and Resources Department of the Government of Yukon. Funding for the remediation is being provided by the Government of Canada.

REGIONAL GEOLOGY

Roddick and Green (1961) first systematically mapped the geology of the Anvil district (1:253,440 scale). Tempelman-Kluit (1972) completed a more detailed geological study after discovery of the Vangorda, Swim, and Faro deposits (1:125 000 scale). More recently Gordey (1983, 2013) and Gordey and Irwin (1987; 1:250 000 scale) correlated Anvil District rock units with rock units previously mapped to the east and southeast. Pigage (2004) integrated the results of company exploration and past government studies with new geological mapping that he completed between 1998 and 2002 (1:25 000 scale). Recently Cobbett (2014, 2015, 2016) has revised Selwyn basin stratigraphy through mapping north and west of the immediate Faro area (1:50 000 scale).

The Anvil district contains the most southwesterly exposures within Selwyn basin (Fig. 1), a large area of central Yukon where carbonaceous clastic rocks accumulated along the ancient North America passive continental margin during Neoproterozoic and early Paleozoic time (Gabrielse, 1967; Gordey and Anderson, 1993). Northeast of Selwyn basin a shallow carbonate platform formed the near-shore facies of the ancient North American margin (Abbott *et al.*, 1986). The Anvil stratiform ore deposits occur within a 150m stratigraphic interval straddling the contact between the Cambrian Mount Mye formation and the Cambrian-Ordovician Vangorda formation (Jennings and Jilson, 1986; Pigage, 1990, 2004).

Anvil district is located immediately northeast of the Yukon-Tanana terrane (Figs. 1 and 2), a middle Paleozoic volcanic arc and associated plutonic assemblage built on continental crust (Mortensen and Jilson, 1985). The Yukon-Tanana terrane rifted away from the continental passive margin forming the Slide Mountain back-arc oceanic basin in Devonian Permian time.

Oblique transpressive collision of Yukon-Tanana terrane with North America in Jurassic through Cretaceous (Mortensen and Jilson, 1985; Colpron *et al.*, 2007) resulted in emplacement of Yukon-Tanana terrane and Slide Mountain oceanic crust structurally on the outer southwest margins of Selwyn basin assemblages. This transpressional collision initiated deformation and metamorphism of the basin. Collsional deformation culminated with the intrusion of mid-Cretaceous granodiorites and granites of the Anvil and Tay River plutonic suites.

Right lateral strike-slip movement along the Tintina fault in Eocene time resulted in at least 430 km of lateral displacement (Gabrielse *et al.*, 2006).

Geographically the area encompassed by Selwyn basin hosts many of Canada's large stratiform lead-zinc deposits, making the Canadian Cordillera a metallogenic province of world-wide significance (Carne and Cathro, 1982). The deposits range in age from Cambrian-Ordovician through Devonian-Permian. The Anvil district is as yet the only producer from stratiform lead-zinc deposits within this area.

DISTRICT STRATIGRAPHY

The stratigraphic sequence of Anvil district ranges from Cambrian to Jurassic in age. The lower Paleozoic part of the sequence is divisible into three major map units (Fig. 3). From the base, these are the Mount Mye formation, the Vangorda formation, and the Menzie Creek formation (Jennings and Jilson, 1986). The aggregate thickness for this succession is approximately 5 km.

The stratiform ore deposits in the Anvil district occur within a 150 m thick sequence that spans the contact between the Mount Mye and Vangorda formations (Jennings and Jilson, 1986). The rest of this section will focus on the above three formations.

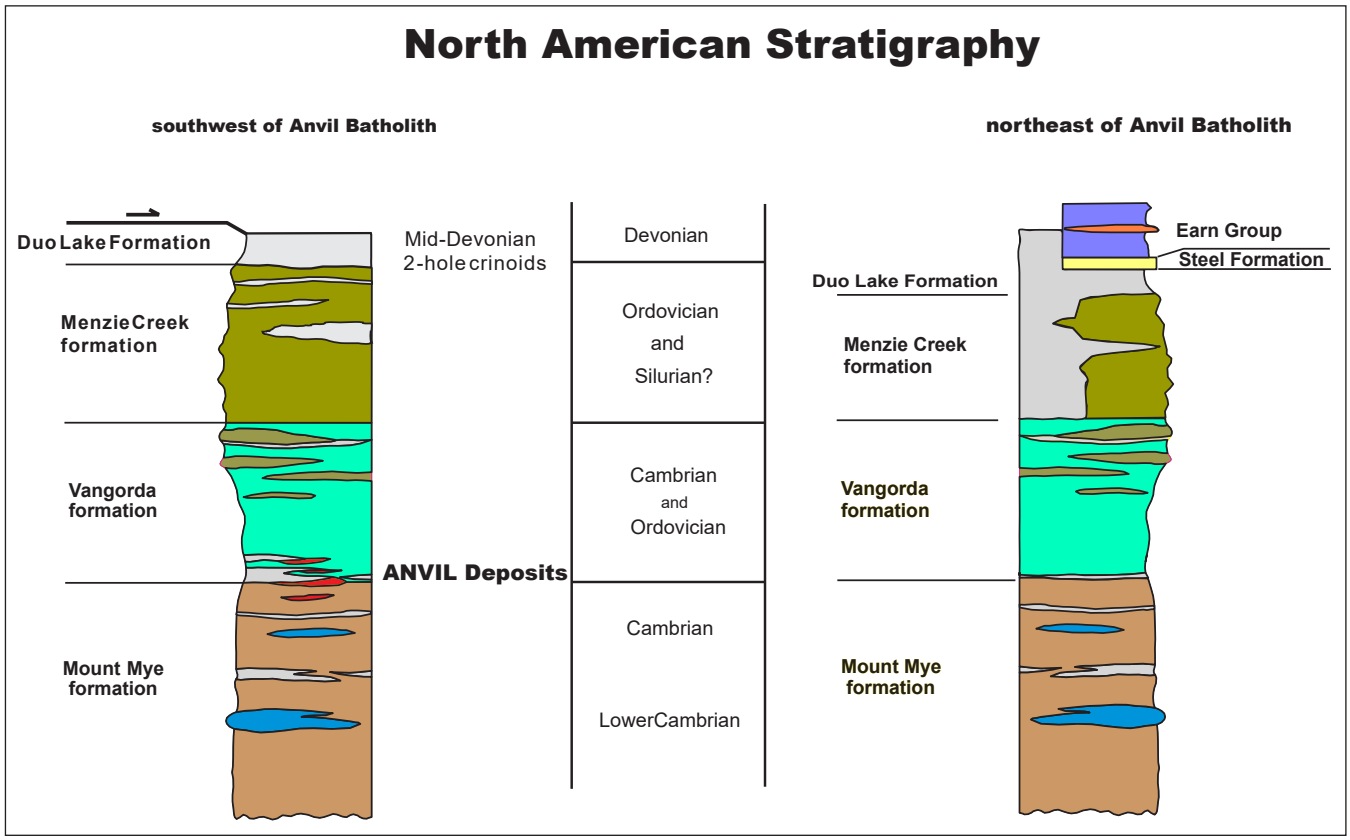

Figure 3. *Lower Paleozoic Anvil District stratigraphy. From Pigage (2004).*

Mount Mye formation

The Mount Mye formation consists primarily of noncalcareous pelite. At lower greenschist facies metamorphic grades the pelite consists of a muscovite-chlorite-quartz phyllite (Fig. 4). At amphibolite facies metamorphic grade it consists of biotite-muscovite-andalusite ± staurolite ± garnet ± fibrolite schist (Fig. 5). Fibrolite is present immediately adjacent to the mid-Cretaceous intrusions of the Anvil plutonic suite. The base of the unit is not exposed in the district. Cross sections on the north side of the Anvil batholith indicate a minimum thickness of approximately 2 km (Pigage, 2004). The upper contact is transitional into the Vangorda formation with interlayering of calcareous and noncalcareous units. The contact is defined as the top of the uppermost substantial noncalcareous phyllite or schist. It locally coincides with the base of a thick carbonaceous, siliceous phyllite or schist in the Vangorda formation.

Figure 4. *Muscovite-chlorite phyllite of the Mount Mye formation. BQ size core from drill hole CNR76-01 (130-137 m). Photo from Pigage (2004).*

Figure 5. *Andalusite-muscovite-biotite schist of the Mount Mye formation. Pencil is 14 cm long. Southwest wall of the Faro open pit. Photo from Pigage (2004).*

The predominant schist or phyllite (80%) is silvery grey with locally developed 1 to 10 cm thick compositional banding in shades of grey and light brown. It weathers with a spotty orange to brown surface coating. Minor pyrite and/or pyrrhotite occur as irregular disseminated grains. Interbands of marble and calc-silicate rock (10%), carbonaceous schist or phyllite (10%), and chloritic phyllite or amphibolite (minor) occur in lesser amounts. Marble within the pelite ranges from white to grey to black. It contains abundant boudins and bands of schist and calc-silicate rock. Calc-silicate rock typically consists of thinly banded light green or cream calc-silicate assemblages and brown pelite assemblages. Banding is irregular and typically on a scale of 1 to 20 cm.

Gordey and Irwin (1987) correlated the Mount Mye formation with the regional Gull Lake Formation (Gordey and Anderson, 1993). Regionally the base of the Gull Lake Formation is a limestone conglomerate which unconformably overlies pelite of the Hyland Group (Gordey and Anderson, 1993; Moynihan, 2014). The limestone conglomerate contains archeocyathids, indicating an early Cambrian age. Regionally the upper Cambrian to late middle Ordovician Rabbitkettle Formation (Gordey and Anderson, 1993) unconformably overlies the Gull Lake Formation, providing a minimum age for the Gull Lake Formation of upper Cambrian. Based on mapping in central Yukon, Moynihan (2014) suggests a minimum age of stage 5 in Cambrian (approximately 504 Ma) for the Gull Lake Formation. Fossils have not been identified within the Mount Mye formation in the Anvil district area.

Detailed geological mapping by exploration geologists in the district was unable to provide evidence for an unconformity at the upper contact of the Mount Mye formation (Jennings and Jilson, 1986; Pigage, 2004). More recently Cobbett (2016) suggests that this upper contact is unconformable based on stratigraphic cutout of sandstone intervals in the upper Mount Mye formation in the vicinity of Tay Mountain.

Vangorda formation

In much of the Anvil district the Vangorda formation (Jennings and Jilson, 1986) consists of pale silvery grey, calcareous, recessive phyllite. At higher metamorphic grade it consists of a resistant, thinly banded, pale cream and dark brown calc-silicate rock. Minor interbedded rock types include limestone or marble, carbonaceous phyllite or schist (10-15%), dolomitic siltstone, and chloritic phyllite or amphibolite (15-20%). Locally the base of the formation contains a mappable carbonaceous phyllite or schist member. Thickness estimates for the entire formation range from 700 to 2200 m (Pigage, 2004).

The Vangorda formation phyllite consists of thinly interbedded medium grey phyllite and light grey calcite-quartz siltstone (Fig. 6). Phyllitic bands are up to 10 cm thick; calcareous siltstone bands range up to 15 cm thick. These thinly interbedded units are intricately folded on a hand sample basis with an axial planar crenulation cleavage (S2) forming the dominant structural foliation surface. Outcrops typically weather with an opaque white, calcareous, drusy surface coating. The phyllite weathers recessively to silvery grey scree slopes.

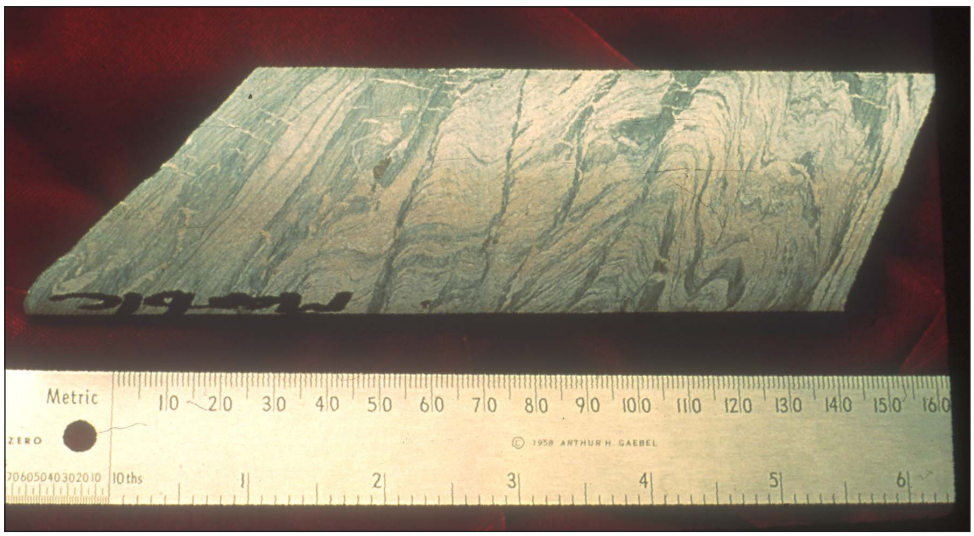

Figure 6. *Muscovite-chlorite phyllite of the Vangorda formation. NQ size core. Pelite bands are silvery-grey and siltstone bands are pale cream and have a grainy texture. Smallest division on scale is 1 mm. Photo from Jennings and Jilson (1986); Pigage (2004).*

At higher metamorphic grades the calcareous phyllite is transformed into a thinly and discontinuously banded green, cream, and purplish brown calc-silicate rock (Fig. 7). The purplish brown bands are the higher metamorphic grade equivalents of the silvery grey phyllitic bands, and the green and cream calc-silicate bands are the higher metamorphic grade equivalents of the calcareous siltstone bands. Outcrops weather as blocky, resistant cliffs with a patchy, opaque white calcite surface coating.

Figure 7. *Calc-silicate rock of the Vangorda formation. Pale green calc-silicate bands and lenses interlayered with dark purplish brown biotite-rich pelite bands. Pencil on right side of photo is 14.5 cm long. Outcrop in southwest wall of Faro deposit open pit. Photo from Pigage (2004).*

Dark grey to black, carbonaceous phyllite to schist horizons occur throughout the formation. Lateral extent and thickness of these horizons is poorly documented. Jennings and Jilson (1986) differentiated a variably siliceous, fine-grained, phyllite to schist at the base of the Vangorda formation as a member because of its great thickness adjacent to some of the massive sulphide ore horizons. It ranges up to 360 m thick and is laterally equivalent to the black, ribbon-banded, quartzose ore facies in the deposits.

White to medium grey, medium to coarsely crystalline marble units ranging from a few metres to tens of metres in thickness occur locally within the Vangorda formation. The marbles typically contain discontinuous bands and lenses of quartz or calc-silicate rock.

The Vangorda formation also contains poorly foliated, fine to medium-grained, dark green to olive green, chloritic phyllite or amphibolite lensoid bodies up to 100 m thick. Laterally these units may extend along strike for several kilometres. They are most common near the top of the formation; they weather as resistant knobs and ridges.

The lower contact of the Vangorda formation with the Mount Mye formation has been discussed above. The upper contact with the Menzie Creek formation is also transitional with interbedding of volcanic rocks and calcareous pelite over a 10 to 30 m interval.

Gordey and Irwin (1987) correlated the Vangorda formation with the regional Rabbitkettle Formation (Gordey and Anderson, 1993). The overlying Menzie Creek formation contains early to middle Ordovician fossils, providing a minimum age for the Vangorda formation. A late Cambrian maximum age is based on regional fossil control from Gull Lake Formation and Rabbitkettle Formation. No fossils have been found in the Vangorda formation.

Menzie Creek formation

The Menzie Creek formation (Jennings and Jilson, 1986) is a thick, resistant, grey-weathering, volcanic unit. Both upper and lower contacts are conformable with interbedding of volcanic rocks with metasedimentary pelite. Thickness varies considerably, ranging from 140 m to possibly as much as 2800 m (Pigage 2004). Primary depositional textures are well preserved northeast of the Anvil batholith; southwest of the batholith the unit consists of a highly foliated, medium green, chloritic phyllite.

Massive and pillowed, locally amygdaloidal flows (Fig. 8) are interbedded with volcaniclastic, monolithic basalt breccia (Fig. 9), conglomerate, sandstone and siltstone. Minor intercalated black phyllite, bedded black chert, calcareous phyllite, limestone and dolostone beds occur throughout the unit.

Figure 8. *Pillow basalt flow in Menzie Creek formation. Field station 99LP258A. Hammer for scale. Photo from Pigage (2004).*

Figure 9. *Matrix supported, monolithic, basalt breccia from Menzie Creek formation. Field station 98LP181. Hammer for scale. Photo from Pigage (2004).*

Discriminant diagrams for the Menzie Creek formation delineate an alkali basalt in a rift-related, within plate tectonic setting (Fig. 10). The multi-element diagram normalized to primitive mantle has an oceanic island basalt (OIB) signature (Fig. 10).

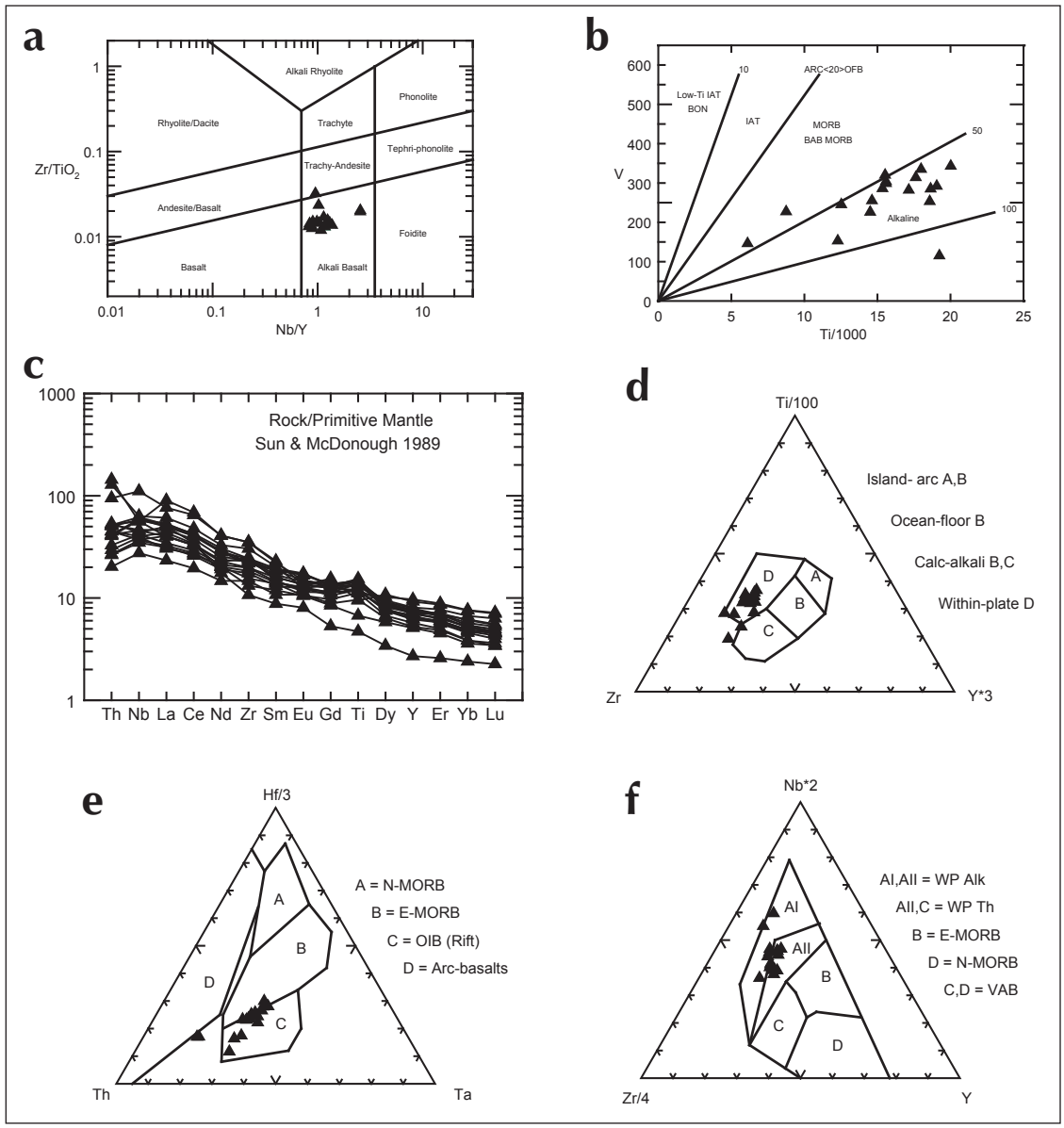

Figure 10. *Composition and tectonic discriminant diagrams for extrusive basalts of the Menzie Creek formation. Modified from Pigage (2004).* ***(a)*** *Zr/TiO2-Nb/Y diagram of Winchester and Floyd (1977) as modified by Pearce (1996);* ***(b)*** *Ti-V diagram of Shervais (1982);* ***(c)*** *primitive mantle normalized multi-element diagram. Primitive mantle values from Sun and McDonough (1989);* ***(d)*** *Zr-Ti-Y diagram of Pearce and Cann (1973);* ***(e)*** *Th-Hf-Ta diagram of Wood (1980); (f) Zr-Nb-Y diagram of Meschede (1986).*

The Menzie Creek formation is the oldest unit in the Anvil district with fossil control. Graptolites and conodonts from the lower to middle part of the unit have an overlapping early Ordovician age. Graptolite fossils from the mainly overlying Duo Lake Formation are middle Ordovician. A suggested middle Ordovician minimum age is feasible.

INTRUSIVE ROCKS

The Lower Paleozoic stratigraphy is intruded by four intrusive suites ranging in age from Ordovician to Eocene. Early Paleozoic gabbro and pyroxenite dikes and sills have exactly the same chemistry as the Menzie Creek volcanics and are interpreted as subvolcanic intrusions.

Three syn to post-metamorphic intermediate to felsic intrusive suites occur as dikes, sills, plugs and major bodies in the Anvil District. The largest intrusive bodies are the Anvil and Orchay batholiths. Pigage and Anderson (1985) informally discussed the medium to coarse-grained mid-Cretaceous intrusions as different phases of the Anvil plutonic suite. Anderson (in Gordey and Anderson, 1993) formally defined the Selwyn Plutonic Suite, encompassing the same units considered as part of the Anvil plutonic suite. More recently Mortensen *et al.* (2000) informally divided the Cretaceous intrusions of the Sewyn Plutonic Suite into different intrusive suites based on age, lithology and geochemistry. This field guide follows the terminology proposed by Mortensen *et al.* (2000).

Ordovician Gabbro and Pyroxenite

Mount Mye, Vangorda and Menzie Creek formations contain gabbro and pyroxenite lenses ranging from a few centimetres up to 100 m in thickness (Fig. 11). Laterally these lenses may be traced along strike for several kilometres. Margins are typically strongly foliated chloritic phyllite. Interiors preserve primary igneous textures. Pyroxenite bodies are variably serpentinized and are commonly magnetic; their magnetic nature results in a false positive massive sulphide signature with magnetic ground and airborne surveys.

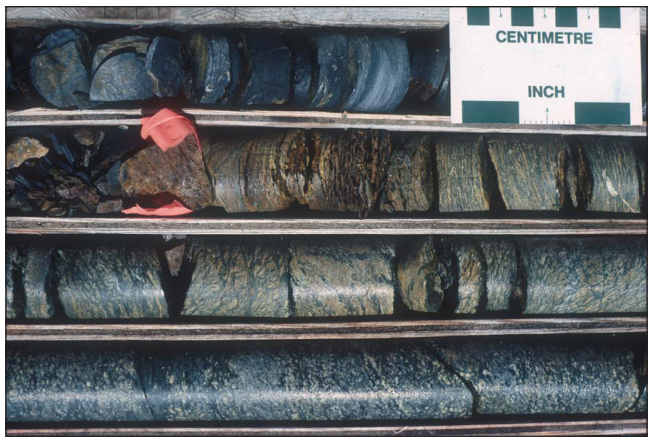

Figure 11. *Ordovician gabbro sill in Vangorda formation. The strongly foliated margin of sill is located immediately to right of flagging. Lower rows are less foliated and display relict igneous texture. BQ size core from drill hole CNR76-04, depth 20–27 m). Photo from Pigage (2004).*

Locally these intrusions have undergone extensive quartz-carbonate alteration, resulting in a rusty weathering, light tan, quartz-carbonate-muscovite rock (Fig. 12). In places these highly altered intrusions contains minor amounts of a bright green layer silicate which has been identified as being a Ni-bearing serpentine mineral (Modene, 1982). The heavily quartz-carbonate altered rocks resemble quartz-carbonate altered mafic and ultramafic igneous rocks described worldwide.

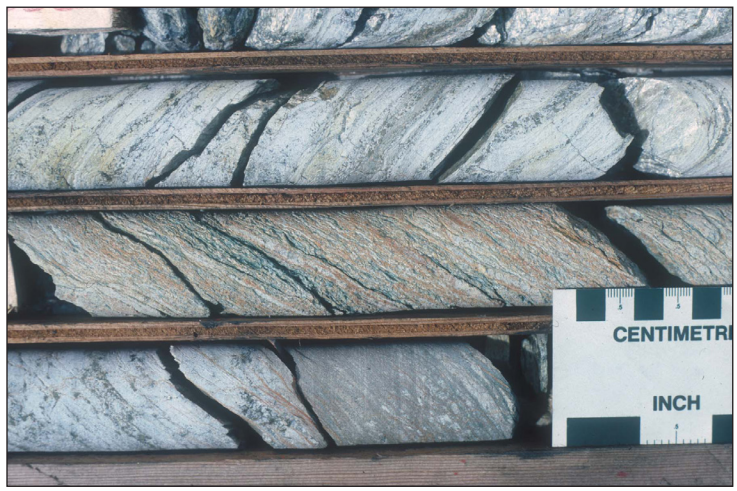

Figure 12. *Strongly quartz-carbonate altered Ordovician gabbro sill in Grum deposit. Sill is strongly foliated and is located in middle row of core. Drill hole FAGU189, 17.9-25 m. BQ size core. Photo from Pigage (2004).*

Discriminant and multi-element normalized diagrams show that the dikes and sills are chemically very similar to the Menzie Creek formation basalt (Pigage, 2004), supporting the interpretation that they are subvolcanic dikes and sills that fed the Menzie Creek volcanic flows.

Cretaceous Anvil plutonic suite

Biotite-muscovite granite (Fig. 13) of the Anvil plutonic suite constitutes the oldest granitic intrusive rocks in the Anvil district (Pigage, 2004). Proportions of biotite and muscovite vary widely. K-feldspar often forms megacrysts. Granitic and aplitic sills occur in the metasedimentary rocks adjacent to the intrusive bodies. Locally, near the margins, the intrusions contain a poorly developed, shallowly dipping foliation fabric defined largely by poorly oriented micas and feldspar megacrysts. The southern edge of the Anvil batholith near the Grum and Vangorda deposits contains a well-developed S-C banding caused by extensional faulting. Metamorphic isograds are concentric around the Anvil batholith.

Figure 13. *Slab of Anvil plutonic suite muscovite-biotite granite. Stained for K-feldspar. Penny is 1.9 cm across. Field station 84-50. Photo from Pigage (2004).*

Two samples, from widely different locations, give U-Pb isotopic crystallization ages of 109 ± 1.2 Ma and 103.9 ± 1.5 Ma on monazite (2 sigma error; Pigage, 2004).

This suite was identified as the Mount Mye phase of the Anvil plutonic suite by Pigage and Anderson (1985). It was mapped as the non-hornblende phase of the Selwyn Plutonic Suite by Gordey and Irwin (1987).

Cretaceous Tay River plutonic suite

The Anvil plutonic suite is intruded by unfoliated biotite ± hornblende granodiorite dikes and sills comprising the Tay River plutonic suite (Mortensen *et al.*, 2000). This suite also occurs as a large intrusive body at the northwest end of the Anvil batholith and constitutes the entire Orchay batholith. It forms a moderately large dike at the northwest end of the Faro deposit open pit (Fig. 14).

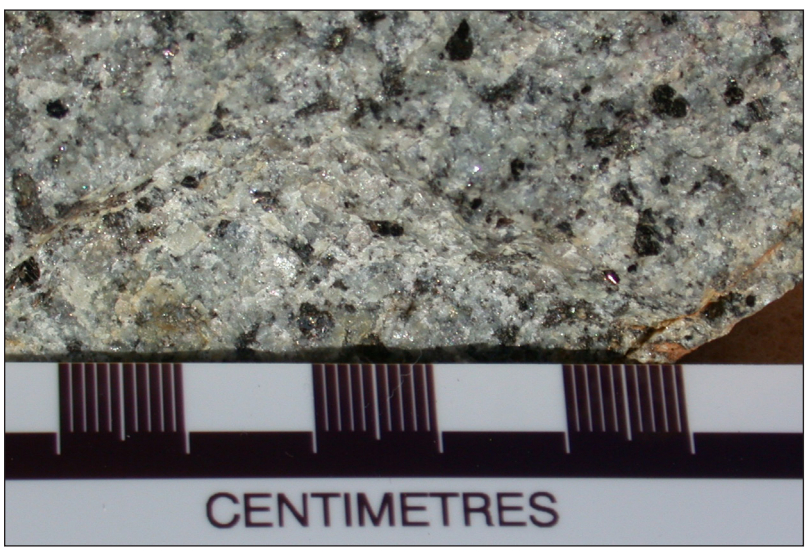

Figure 14. *Biotite granitoid of the Tay River plutonic suite. Sample from northwest wall of the Faro open pit. Photo from Pigage (2004).*

Marginal contacts are sharp and crosscut compositional layering. Locally the intrusions contain a fine-grained marginal phase with large, dark green hornblende and smaller white plagioclase phenocrysts in a pale greenish grey matrix. Pelite immediately adjacent to the Tay River intrusions is typically hornfelsed.

Pigage and Anderson (1985) described and classified this unit as the Orchay phase of the Anvil plutonic suite. Gordey and Irwin (1987) denoted it as the hornblende-bearing phase of the Selwyn Plutonic Suite.

U-Pb isotopic ages on monazite and zircon give crystallization ages tightly clustered between 98.6 ± 0.2 Ma and 95.3 ± 1.3 Ma (Pigage, 2004). Similar chemistry and isotopic ages for the South Fork volcanics indicate the intrusive suite forms the subvolcanic equivalents for the South Fork rocks (Pigage, 2004).

Eocene quartz-feldspar porphyry

Small opaque-white weathering, aphanitic feldspar porphyry dikes and plugs (Figs. 15 and 16) are scattered throughout the area. The porphyry contains sparse white K-feldspar phenocrysts and abundant smokey grey and clear quartz phenocrysts. Samples of this intrusive suite are noted in the Faro pit waste dumps.

U-Pb isotopic dates on zircon result in dates of 55.8±0.1 Ma and 53.8±0.2 Ma (Pigage, 2004). K-Ar and Ar-Ar whole rock dates fit within this same general age interval (Gordey, 2013).

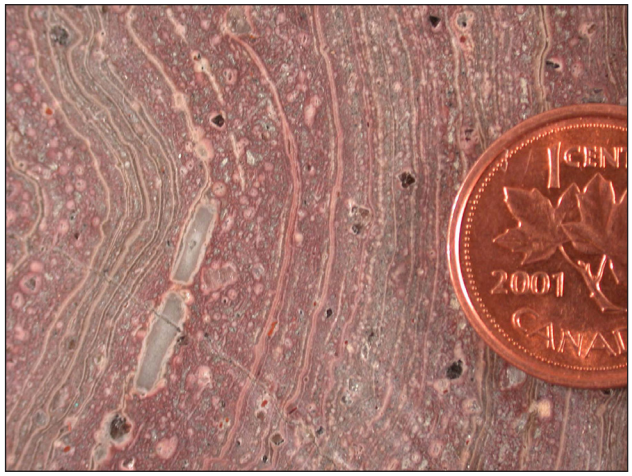

Figure 15. *Eocene quartz-feldspar porphyry. Flow-banded with scattered clear and grey quartz phenocrysts. Field station 99LP228. Penny is 1.9 cm across. Photo from Pigage (2004).*

Figure 16. *Eocene quartz-feldspar porphyry. Smokey quartz and small white feldspar phenocrysts. Sample from northeast wall of Faro open pit. Penny is 1.9 cm across. Photo from Pigage (2004).*

DEFORMATION

Five phases of deformation have been recognized within the Anvil District (Jennings and Jilson, 1986). The first two are regionally developed as intense Mesozoic contractional deformations with concurrent metamorphism; these determine the gross structure of the mineral deposits. The remaining deformation phases are only locally developed and do not generally form large or significant structures.

D1 (S1) Deformation

Small, northeast-verging, asymmetric, upright folds with associated pervasive axial planar cleavage related to the D1 deformation are rarely preserved in the District. They trend northwest and plunge gently to the northwest or southeast. Rarely they are visible in drill

core (Fig. 17) and outcrop (Fig. 18). More commonly the D1 deformation fabric consists of microlithons within the phase 2 deformation (D2) spaced axial planar crenulation cleavage. Primary bedding S0 has been transposed into near parallelism with the S1 foliation.

Figure 17. *D1 minor fold defined by siltstone bed in Vangorda formation. Drill hole 76X-11 (22 m). NQ size core. Photo from Pigage (2004).*

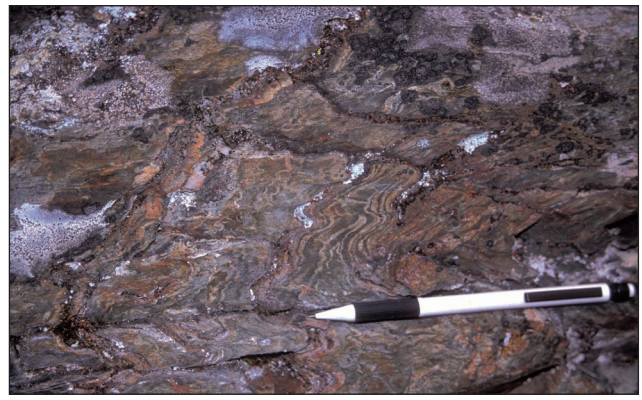

Figure 18. *Small D1 fold in Vangorda formation adjacent to Ordovician gabbro sill. Pencil is 14 cm long. Photo from Pigage (2004).*

D2 (S2) Deformation

D2 deformation is manifested by a gently dipping axial planar crenulation cleavage (S2), forming the dominant structural fabric within the Anvil district. The S2 cleavage is domed over the northwest-trending Anvil Arch which is centred over the Anvil batholith (Tempelman-Kluit, 1972); southwest of the arch axis the S2 foliation largely dips gently to the southwest, and northeast of the arch axis it dips predominantly gently to the northeast. Intensity of the S2 fabric decreases with increasing lateral distance from the Anvil arch axis.

D2 minor folds are pervasive on the southwest side of the Anvil batholith in the vicinity of the stratiform mineral deposits. The D2 minor folds are asymmetric with long upright limbs and short steep to inverted limbs. D2 folds are common on an outcrop scale (Fig. 19) and are readily visible in drill core (Fig. 20). Southwest of the Anvil batholith D2 folds verge southwest; northeast of the Anvil batholith they verge to the northeast.

Figure 19. *Small D2 fold in Vangorda formation phyllite. Coin is 2.7 cm wide. Photo from Pigage (2004).*

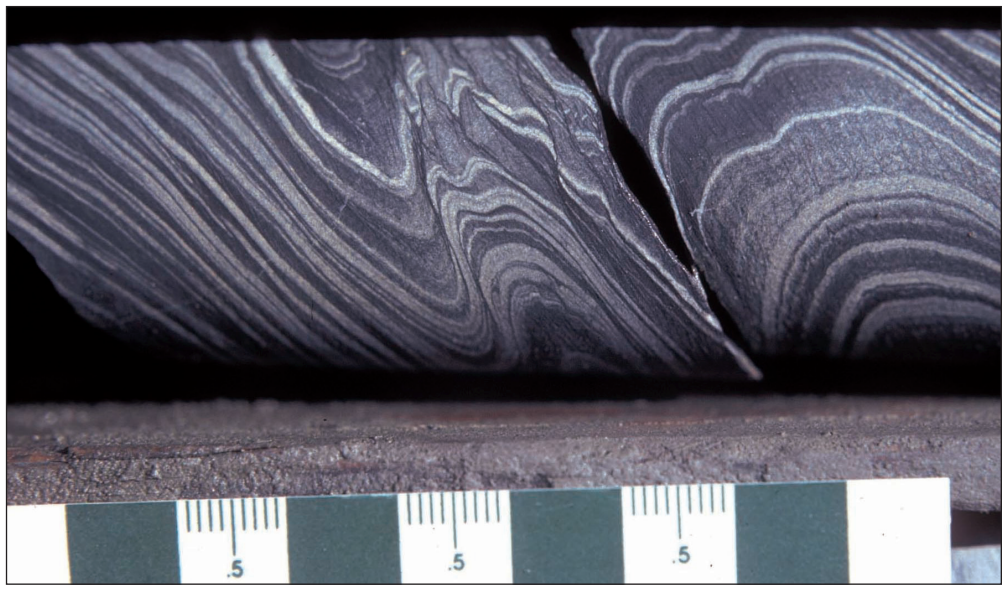

Figure 20. *D2 minor fold in Vangorda formation. NQ size core. Drill hole &2X-23, 26 m depth. Photo from Pigage (2004).*

Locally developed incipient structural fabrics in the margins of the Anvil plutonic suite indicates the time of D2 deformation approximately correlates with mid-Cretaceous intrusion of the two-mica granites.

Regional scale extensional faults on the southwest side of the Anvil batholith have been delineated by detailed geological mapping (Pigage and Jilson, 1985). These faults have had a major effect on structural position of the deposits relative to the current erosion surface. They are also major factors in limiting the extent of the deposits laterally. The best documented of these faults is the Tie fault which truncates the northwest extension of the Grum deposit. The Tie fault has been mapped for a strike length of 6 km, is up to 150 m thick, and has a minimum displacement of 1 km on the fault surface. On the margins of the batholith, S-C banding texture on the southwest margin of the Anvil batholith (Fig. 21) and shear bands in the adjacent phyllite marks the trace of

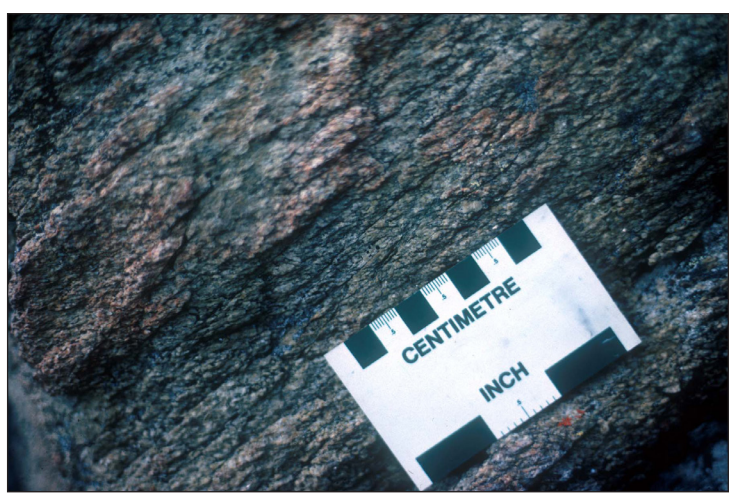

Figure 21. *S-C banding in outcrop of Anvil plutonic suite in the immediate footwall of the Tie fault. C-bands are parallel to the edge of the scale card. Field station 84-4. Photo from Pigage (2004).*

the fault. The extensional faults are clearly post-metamorphic in that they displace the concentric isograds along the southwest margin of the batholith. However, shear band textures within the fault zones have the same orientation as the S2 crenulation cleavage in rocks adjacent to the fault zones. These different relationships indicate the extensional faults represent the last deformation event related to the D2 deformation.

Crystallization ages for the Anvil plutonic suite denote the approximate time of D2 deformation and M2 metamorphism. Tay River plutonic suite intrusions are unfoliated and do not contain any extensional fault shearing textures, even when the intrusions are within the fault zone. Crystallization ages for the Tay River suite therefore post-date the time of peak D2 deformation and M2 metamorphism. D2 deformation is constrained to the approximate time interval of 109 Ma to 99 Ma.

METAMORPHISM

Metamorphism was concurrent with D1 and D2 deformation. Pelite metamorphic mineral assemblages range from muscovite-chlorite zone in greenschist facies to sillimanite-muscovite zone in amphibolite facies. Brown (1994) determined that chlorite compositions in S1 and S2 structural fabrics have identical compositions; he concluded that D1 deformation and M1 metamorphism have been penetratively overprinted by D2 deformation and M2 metamorphism. This corroborates inclusion trail studies by Smith and Erdmer (1990) indicating that only biotite recognizably grew during M1 metamorphism; all other pelite metamorphic minerals grew or recrystallized during various stages of M2/D2 metamorphism and deformation.

Smith and Erdmer (1990) mapped biotite in, andalusite in or out, staurolite in or out, garnet in, and sillimanite in isograds forming a concentric pattern around the Anvil batholith. The isograds are well constrained along the northeast and east margins of the batholith. Along the southwest margin the isograds are cut out by the extensional Tie fault which juxtaposes lower grade rock against the batholith margin.

A pressure near 3 kbars with temperatures ranging from 400-620°C is indicated by comparing mineral assemblages to a pelite petrogenetic grid (Smith and Erdmer, 1990). Using the plagioclase-garnet-Al_2SiO_5-quartz geobarometer and garnet-biotite geothermometer calibration resulted in a pressure near 4.9 kbars with temperatures ranging from 509 to 872°C (Smith and Erdmer, 1990).

Chlorite geothermometry and sulphide thermobarometry in the immediate vicinity of the Vangorda deposit (muscovite-chlorite zone) resulted in a mean temperature range of 336 to 363°C and a mean pressure of 4.0 to 6 kbars (Brown, 1994). These results are reasonably consistent with those of Smith and Erdmer.

STRATIFORM ZINC-LEAD-SILVER SEDEX MINERALIZATION

The Anvil district stratiform ore deposits are confined to an approximately 150 m thick interval encompassing the contact between the Mount Mye and Vangorda formations. This stratigraphic position suggests the deposits are late Cambrian in age (about 490 Ma; Cohen *et al.*, 2015). The deposits consist of up to five sheets of sulphide mineralization within interbedded sedimentary rocks. For deposits containing several horizons, the horizons are generally stacked one above the other. At least three of the horizons appear to be laterally equivalent to the thick basal carbonaceous phyllite member of the Vangorda formation. Detailed mapping and drilling suggests the deposits occur close to a northeasterly zero edge of the carbonaceous basal Vangorda formation member.

All deposits contain a limited number of different ore types. Broadly speaking, these ore types are divided into quartzose disseminated sulphides, pyritic and baritic sulphides. Quartzose sulphides may be either carbonaceous or noncarbonaceous. All of the ore types are completely recrystallized metamorphic tectonites containing S1 and S2 foliations.

The massive pyritic sulphides consist of massive to banded, usually weakly foliated pyrite with lesser sphalerite and galena (Fig. 22). Total sulphide content is at least 60%. Quartz, barite, and carbonate are typical gangue minerals. A variant of this rock type (Fig. 23) consists of porphyroblasts of pyrite in a matrix of dark reddish brown to black galena and sphalerite (buckshot facies).

The baritic massive sulphide ore type (Fig. 24) is strongly and thinly banded. Pyrite, galena, sphalerite and magnetite are disseminated in a gangue of off-white barite and carbonate. Barite content ranges up to 50%. There is a complete gradation between baritic sulphides and pyritic sulphides. Lead + zinc grade is typically high. Sphalerite is characteristically honey-coloured to reddish brown.

Pyrrhotitic massive sulphides consist of massive, finely crystalline, foliated pyrrhotite with less than 50% pyrite and variable amounts of sphalerite and galena with minor chalcopyrite. In the Vangorda deposit this ore type typically occurs at lithofacies contacts between ore types and along the limbs of

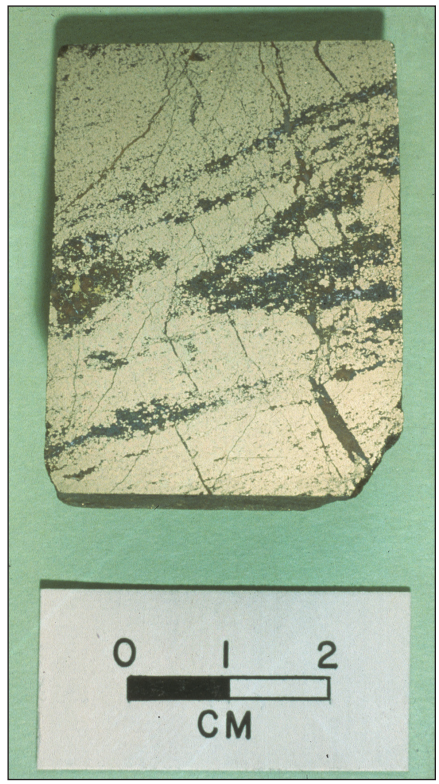

Figure 22. *Banded pyritic massive sulphides sample, Swim deposit. Photo from Jennings and Jilson (1986).*

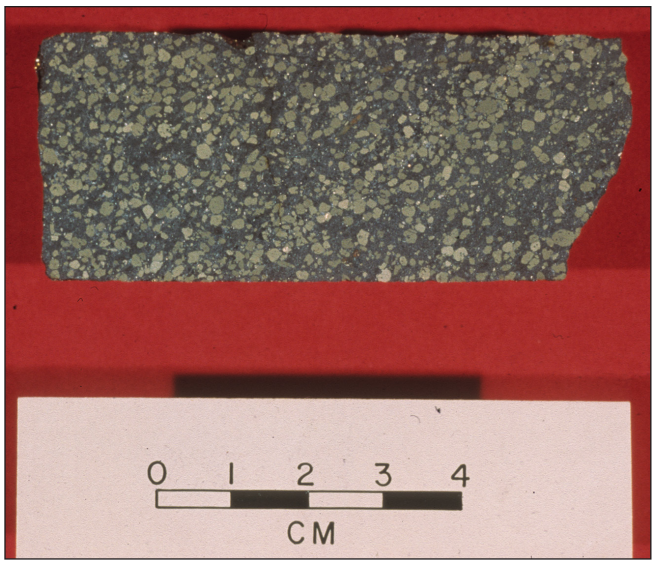

Figure 23. *"Buckshot" high grade pyritic massive sulphides, Faro deposit. Photo from Jennings and Jilson (1986).*

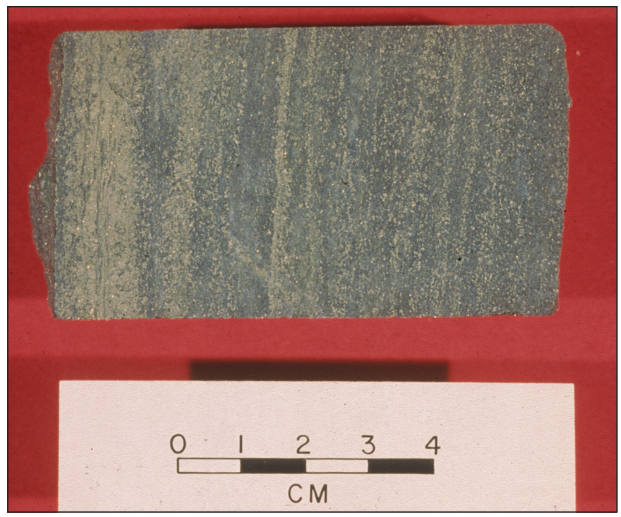

Figure 24. *Baritic massive pyritic sulphide sample, Dy deposit. Photo from Jennings and Jilson (1986).*

D2 folds (Brown and McClay, 1994). Typically it forms flattened lenses elongate within the S2 foliation. Numerous shear indicators within the sulphide matrix attest to extensive shear strain.

Quartzose sulphides typically are fine grained, siliceous with sulphides disseminated through the silica or as quartz-sulphide veinlets. There is a continuous variation from a dark grey to black carbonaceous variant called ribbon-banded graphitic pyritic quartzite (Fig. 25) to an off white to cream pyritic quartzite. Banding is on a scale of 0.2 to 2.0 cm. Total sulphide content is highly variable. Microlithon textures with folded quartz-sulphide veinlets are common.

Figure 25. *Ribbon-banded, graphitic quartzose ore sample, Dy deposit. Photo from Jennings and Jilson (1986).*

In the Faro deposit, the northeast edge contains of thick interval of low grade to barren pyritic quartzite (Fig. 26) with elevated copper content and more abundant magnetite. A similar facies is developed in the footwall of the Vangorda deposit. At Vangorda, this pyritic quartzite is gold rich (1 g/t).

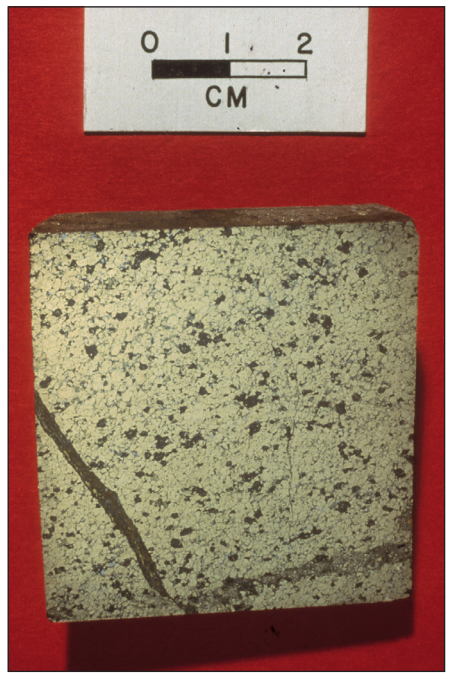

Figure 26. *Homogeneous, foliated, pyritic massive sulphide, Faro deposit. Photo from Jennings and Jilson (1986).*

IDEALIZE ANVIL DEPOSIT (ANVIL CYCLE)

The five deposits have a common arrangement of the sulphide ore types vertically and laterally. Jennings and Jilson (1986) in describing this arrangement termed it the Anvil Cycle (Fig 27). The Anvil cycle is based largely on mineralization in the Faro and Vangorda deposits.

The base of the cycle consists of ribbon-banded carbonaceous quartzose sulphides. Laterally these sulphides grade into siliceous carbonaceous phyllite. Vertically the graphitic sulphides are overlain by pyritic quartzite, siliceous pyritic sulphides, pyritic massive sulphides and baritic massive sulphides. Informally the succession has the appearance of a fried egg with the yolk being represented by the baritic sulphides.

Anvil cycles are developed on widely varying scales and to different degrees of completeness. This facies zoning can be used in a careful way as tops indicators for stratigraphic facings within the mineralization.

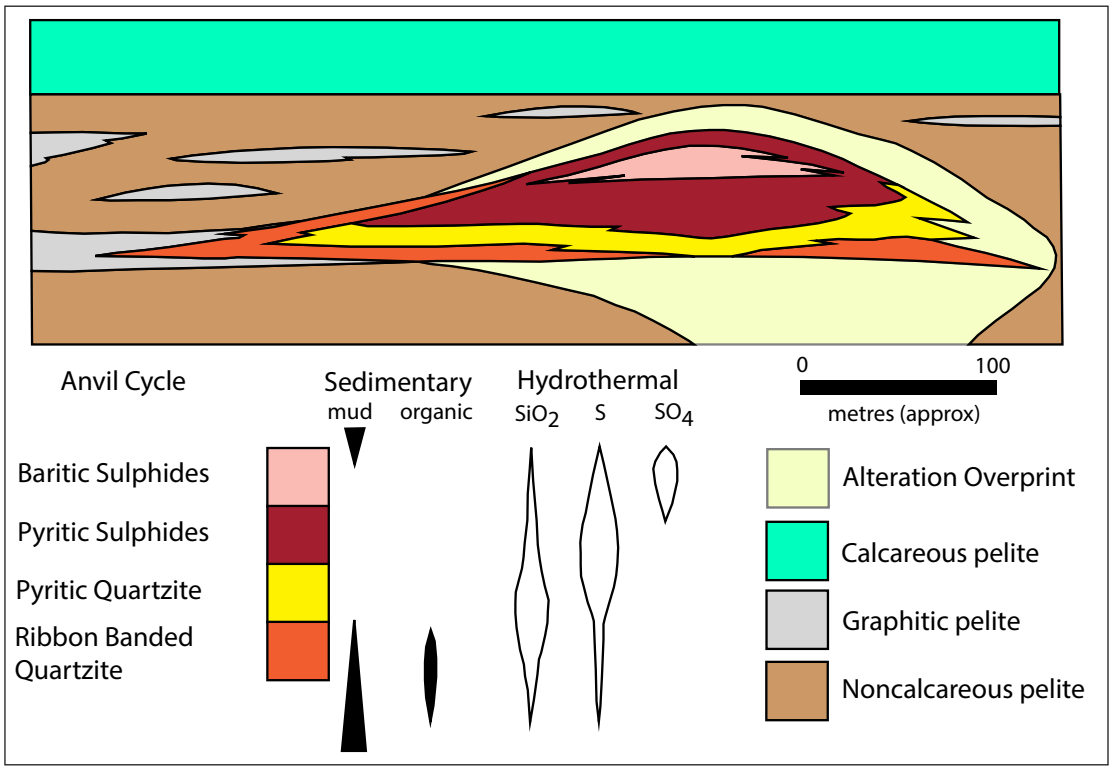

Figure 27. *Idealized Anvil cycle displaying typical distribution of ore facies within the stratiform deposits, based largely on Faro and Vangorda deposits. From Jennings and Jilson (1986).*

ALTERATION

Alteration of enclosing host phyllite is predominantly in the footwall but also includes a small envelope in the hanging wall. Weak alteration consists of thin chloritic veinlets, often with fine disseminated pyrrhotite, quartz, carbonate and minor chalcopyrite. More intense alteration results in a pervasive overprint consisting of quartz and muscovite.

No unequivocal feeder zone has been recognized in association with the deposits.

VANGORDA DEPOSIT

The Vangorda deposit was the initial discovery in the area. The deposit was drilled off by Prospectors Airways. In 1979 the deposit was purchased by Cyprus Anvil Mining Corporation. Curragh Resources acquired the deposit in 1985. Production from the deposit occurred between 1990 and 1993.

The deposit subcrops beneath glacial till. It has been traced over a surface area of 1300 by 200 m. It is elongate in a northwest trending direction. The deposit occurs in the noncalcareous muscovite-chlorite phyllite of the Mount Mye formation structurally about 50 to 120 m beneath the Vangorda formation.

Figures 28 and 29 contain plan and vertical cross section views of the deposit, respectively. A steep extensional fault truncates the deposit at its northwest end. The deposit is divided into several structural domains by extensional faults. The most extensive and highest grade part of the deposit occurs between the Northwest fault and the Cross fault.

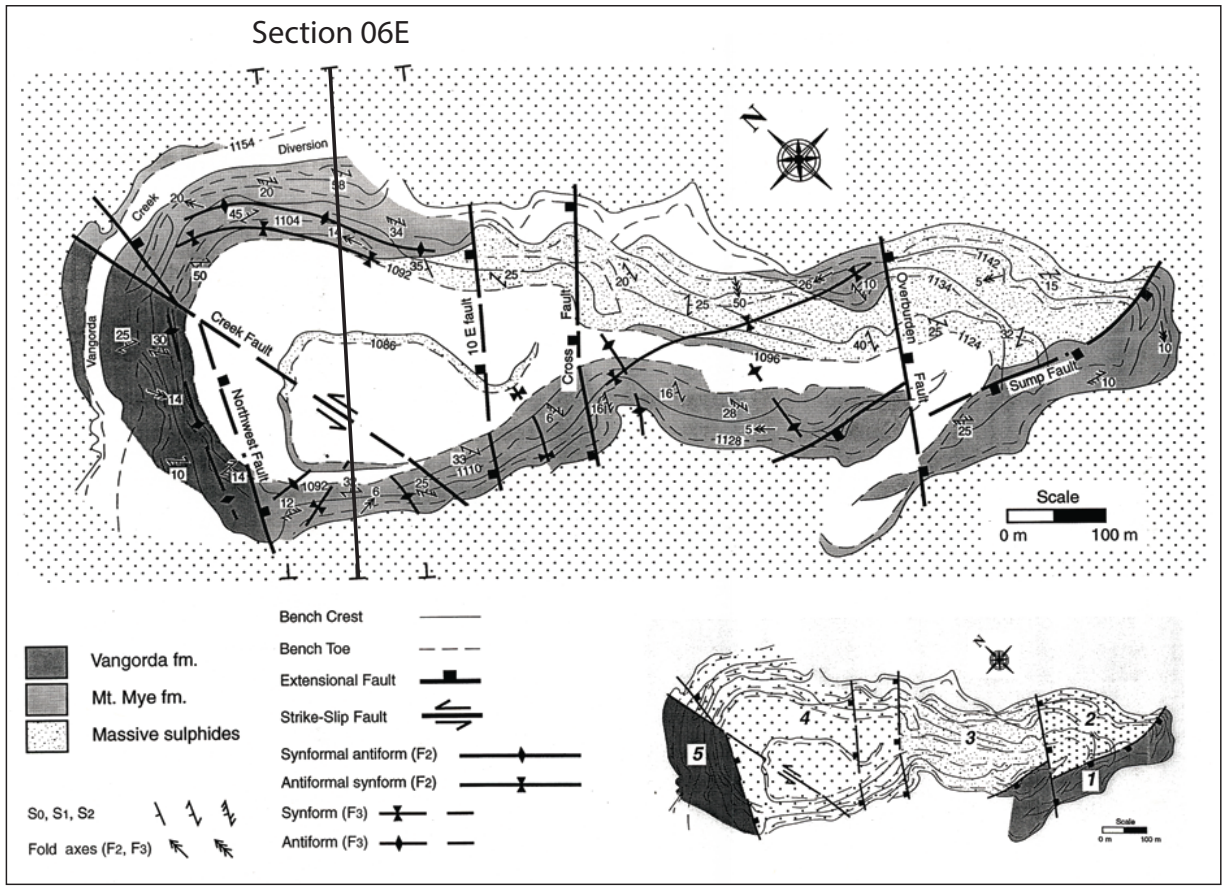

Figure 28. *Vangorda deposit pit map. Location of vertical section 06E is indicated. Modified from Brown and McClay (1994).*

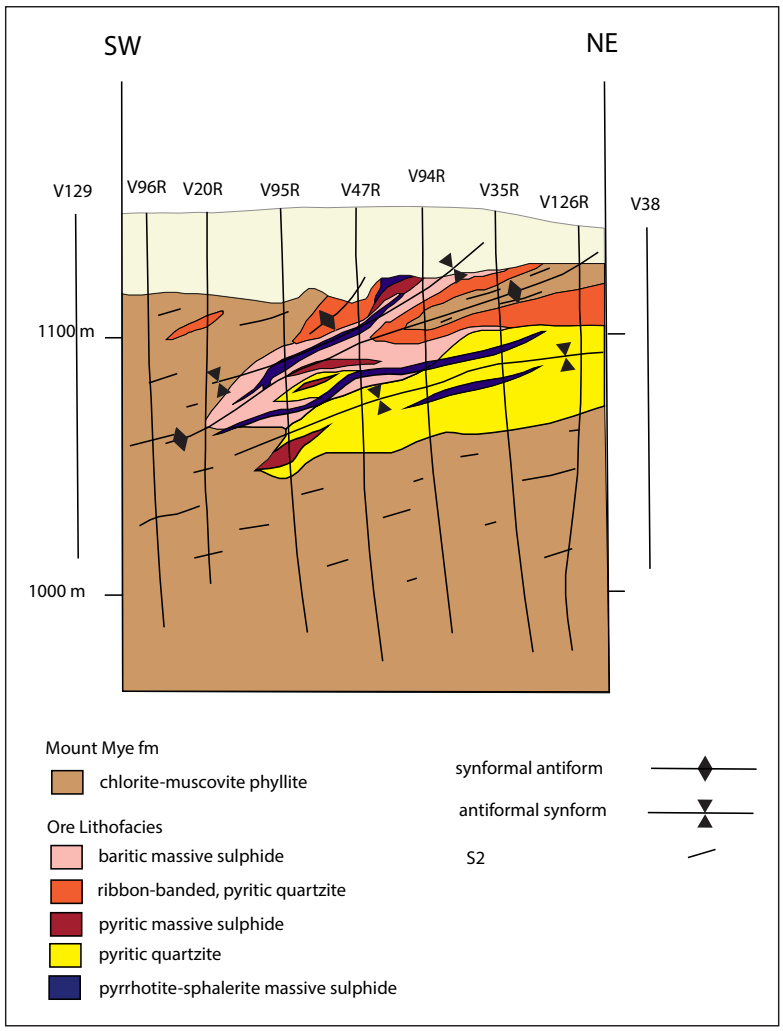

Figure 29. *Vertical cross section 06E, Vangorda deposit. Core from 79V047R was viewed in the Bostock Core Library yesterday. Modified from Brown (1993).*

GRUM DEPOSIT

The Grum deposit was discovered in 1973 by Aero Aho (AEX Minerals in joint venture with Kerr Addison) through drill testing a gravity anomaly. Stripping of the Grum deposit began in 1993. Production ended in 1998 with Anvil Range Mining Corp going into receivership. Much of the deposit is still present beneath the present pit surface.

The deposit subcrops beneath till and glaciofluvial sediments. Overburden is thin to absent in the northwest and thickens to 100 m toward the southeast.

It consists of 3 to 5 stratiform ore horizons in lower Vangorda and upper Mount Mye formations. The most important horizon occurs immediately at the Vangorda-Mount Mye contact. Carbonaceous phyllite of the basal Vangorda member is well developed

in the immediate deposit area. Metamorphic grade is muscovite-chlorite zone in greenschist facies. Quartzose ore types constitute about 50% of the deposit.

Ore horizons define a type-3 interference pattern (Ramsay, 1967) with upright, asymmetric, northeast verging D1 folds refolded by a gently southwest dipping, southwest verging D2 folds (Fig. 30). Both D1 and D2 folds plunge gently to the northwest. The northwest extension of the deposit is truncated by the Tie fault.

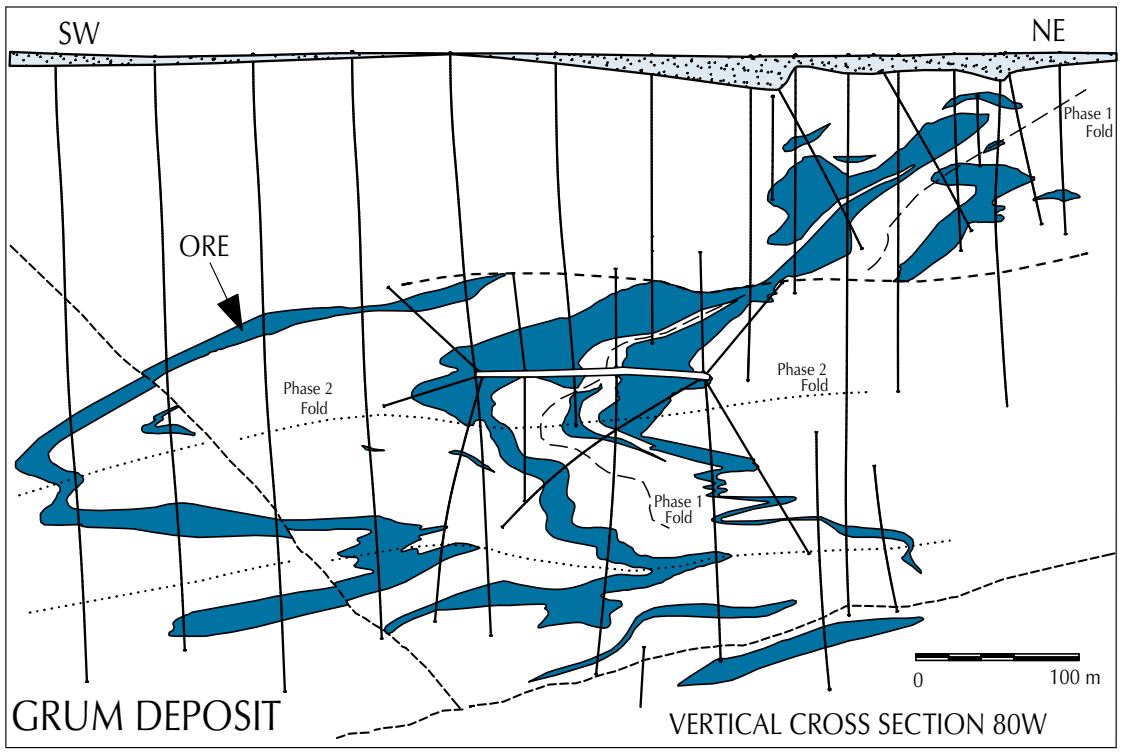

Figure 30. *Vertical cross section 80W through the Grum deposit. Figure from Pigage (2004).*

FARO DEPOSIT

The Faro deposit was discovered in 1964 by Dynasty Exploration through drill testing a geophysical anomaly. Interestingly the discovery drill hole was completed on open ground because of claims being staked in the wrong location. Production ceased in 1993 as the open pit was needed as a tailings repository.

The deposit occurs in biotite-muscovite-andalusite schist of the Mount Mye formation, about 100 m structurally beneath the Vangorda formation. Tay plutonic suite and Eocene porphyry intrusions occur as dikes within and adjacent to the deposit. Because of the higher metamorphic grade, the Vangorda formation consists of hard, dense, banded calc-silicate rock.

Dimensions before mining were 2000 m strike length, 800 m width, and about 70 m thick. It is a flat lying, elongate lens with a thick northeast side and a thin tapering southwest side. Mineralization consists of a massive sulphide and baritic sulphide core surrounding by quartzose variably carbonaceous ores laterally and vertically (Fig. 31). The northeast edge of the deposit consists of an extensive very low grade, semi-massive pyritic quartzite zone. Extensional faults have divided the deposit into three zones. Zone 1 (northwest end) was mined first, and zone 2 (southeast end) was mined next. The middle zone 3 was the deepest and was mined last.

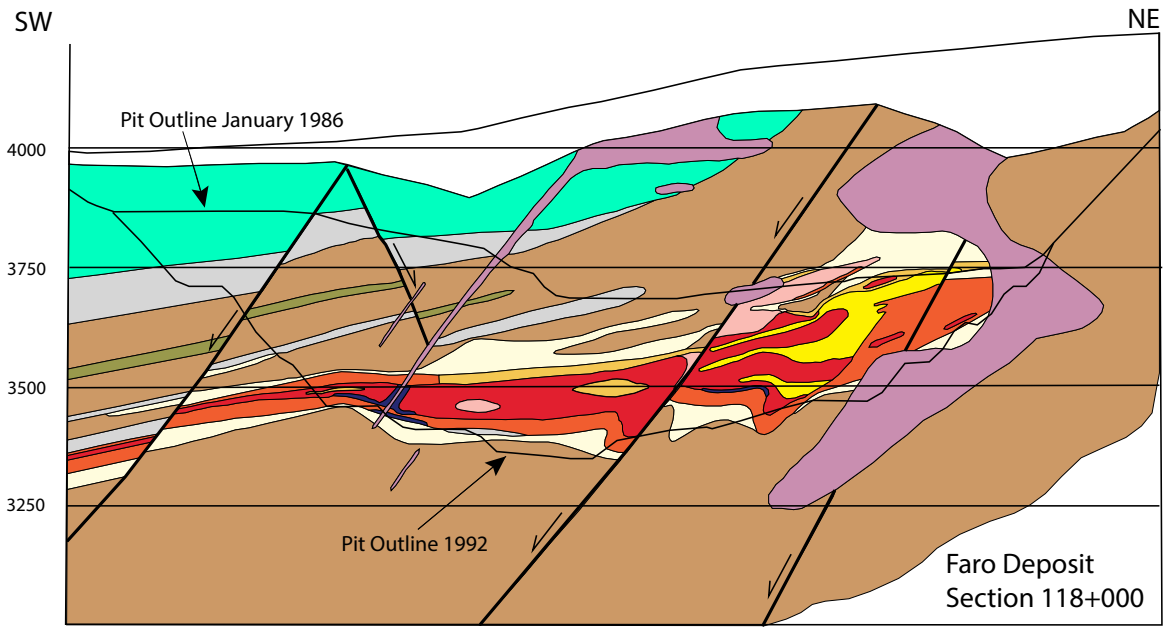

Figure 31. *Vertical cross section 118 through the Faro deposit.*

Bostock Core Library

NQ core from drill hole 79V47R – Section 06E – Vangorda deposit

From (ft)	To (ft)	Interval (ft)	Lithology	Note
0.0	33.7	33.7	#	TRICONED NO CORE overburden
33.7	40.5	6.8	4A0	quartzose ore - ribbon banded graphitic
40.5	42.1	1.6	4G0	baritic massive sulphides
42.1	43.1	1.0	4FEK	carbonate bearing massive pyritic sulphides
43.1	43.9	0.8	4EK	carbonate bearing massive pyritic sulphides
43.9	45.7	1.8	4G8	magnetite bearing baritic massive sulphides
45.7	48.2	2.5	4L37	calcareous, chloritic altered phyllite
48.2	49.0	0.8	4G8	magnetite bearing baritic massive sulphides
49.0	50.0	1.0	4L0	altered phyllite
50.0	52.0	2.0	4E0	low grade pyritic massive sulphides
52.0	54.4	2.4	4G8	magnetite bearing baritic massive sulphides
54.4	55.3	0.9	5D6	noncalcareous chloritic phyllite
55.3	57.5	2.2	4E0	low grade pyritic massive sulphides
57.5	62.1	4.6	4G8	magnetite bearing baritic massive sulphides
62.1	63.0	0.9	4L1	siliceous altered phyllite
63.0	64.8	1.8	4E8	magnetite bearing pyritic massive sulphides
64.8	68.9	4.1	4C0	low grade quartzose ore
68.9	77.8	8.9	4C0	low grade quartzose ore
77.8	79.6	1.8	4C0	low grade quartzose ore
79.6	86.0	6.4	4C8	magnetite bearing low grade quartzose ore
86.0	86.1	0.1	5D0	chloritic phyllite
86.1	87.8	1.7	4D07	quartzose ore -
87.8	93.1	5.3	4C0	low grade quartzose ore
93.1	95.9	2.8	4L0	altered phyllite
95.9	103.0	7.1	4L0	altered phyllite
103.0	106.7	3.7	4L0	altered phyllite
106.7	112.8	6.1	5B2	dark grey phyllite

From (ft)	To (ft)	Interval (ft)	Lithology	Note
112.8	117.0	4.2	4L3	calcareous altered phyllite
117.0	127.7	10.7	4L67	noncalcareous, chloritic altered phyllite
127.7	136.7	9.0	4L7691	noncalcareous, siliceous, chloritic altered phyllite
136.7	139.6	2.9	4L1796	noncalcareous, siliceous, chloritic altered phyllite
139.6	148.7	9.1	5B619	noncalcareous, siliceous, phyllite
148.7	154.8	6.1	4L67	noncalcareous, chloritic altered phyllite
154.8	156.6	1.8	4L3	calcareous altered phyllite
156.6	156.9	0.3	GOUGE	fault gouge
156.9	160.9	4.0	4L0	altered phyllite
160.9	162.2	1.3	4A0	quartzose ore - ribbon banded graphitic
162.2	163.4	1.2	4K0	carbonate bearing massive pyritic sulphides
163.4	176.8	13.4	GOUGE	fault gouge

From (ft)	To (ft)	Intvl (ft)	Recov (ft)	Recov (%)	Sample No	Lithology	Rock Code (numeric)	SG pulp	Pb+Zn (%)	Pb (%)	Zn (%)	Zn/ (Pb+Zn)	Ag-AA (g/t)	Ag-FA (g/t)	Au (g/t)	Po+Py (%)	Po (Sol Fe) (%)	Py (Insol Fe) (%)	BaO (%)	Cu (%)	Hg (%)	Mn (%)
0.0	33.7	33.7	-1	-1	0	WASTE	0	-1	-1	-1	-1	-1	-1	-1	-1	-1	-1	-1	-1	-1	-1	-1
33.7	35.1	1.4	1.3	92	103199	4A0	20	2.69	4.01	1.36	2.65	0.66	21.0	20.0	0.69	7.90	1.20	6.70	0.30	0.08	0.002	0.03
35.1	36.6	1.5	1.5	100	103200	4A0	20	2.86	6.82	3.30	3.52	0.52	49.0	47.0	0.96	10.00	1.20	8.80	0.15	0.04	0.002	0.02
36.6	38.1	1.5	1.5	100	103301	4A0	20	2.88	7.06	3.24	3.82	0.54	47.0	-1.0	0.31	7.50	1.30	6.20	0.20	0.05	0.002	0.03
38.1	39.6	1.5	1.5	100	103302	4A0	20	3.02	10.02	4.62	5.40	0.54	64.0	-1.0	0.75	10.90	1.60	9.30	0.45	0.06	0.002	0.03
39.6	40.5	0.9	0.9	99	103303	4A0	20	3.22	10.52	4.38	6.14	0.58	69.0	-1.0	0.58	12.70	2.40	10.30	2.30	0.07	0.002	0.1
40.5	42.1	1.6	1.5	93	103304	4G0	60	4.25	11.81	5.04	6.77	0.57	82.0	-1.0	0.96	21.20	2.60	18.60	12.53	0.13	0.002	0.19
42.1	43.6	1.5	1.5	100	103305	4EFK	50	4.38	8.02	3.98	4.04	0.50	54.0	-1.0	1.47	28.40	4.70	23.70	5.01	0.16	0.002	0.4
43.6	45.1	1.5	1.5	100	103306	4G8/E	60	4.56	8.37	3.16	5.21	0.62	54.0	-1.0	0.99	22.90	5.50	17.40	14.74	0.12	0.002	0.57
45.1	45.7	0.6	0.6	99	103307	4G8	60	4.42	18.11	9.93	8.18	0.45	130.0	-1.0	0.58	21.60	10.00	11.60	8.37	0.05	0.002	1.52
45.7	48.2	2.5	2.4	96	103308	4L37	120	3.03	2.02	0.98	1.04	0.51	18.0	15.0	0.27	9.50	4.80	4.70	4.99	0.05	0.002	0.2
48.2	49.0	0.8	0.8	100	103309	4G8	60	4.85	11.77	5.16	6.61	0.56	92.0	88.0	0.72	17.00	1.60	15.40	24.09	0.09	0.002	0.1
49.0	50.0	1.0	1.0	100	103310	4L0	120	3.45	7.23	3.30	3.93	0.54	58.0	52.0	0.34	11.30	4.30	7.00	9.67	0.03	0.002	0.26
50.0	52.0	2.0	2.0	100	103311	4E0	50	4.52	6.74	2.96	3.78	0.56	52.0	49.0	0.86	27.00	1.80	25.20	7.00	0.04	0.003	0.11
52.0	53.2	1.2	1.2	99	103312	4G8	60	4.75	10.88	3.66	7.22	0.66	61.0	58.0	0.24	16.40	1.30	15.10	26.98	0.04	0.003	0.17
53.2	54.4	1.2	1.2	99	103313	4G8	60	4.51	9.32	2.88	6.44	0.69	55.0	52.0	0.24	13.10	4.20	8.90	30.52	0.02	0.002	0.8
54.4	55.9	1.5	1.5	100	103314	4E/5D	50	3.94	12.40	5.06	7.34	0.59	72.0	72.0	0.58	17.20	3.10	14.10	11.08	0.07	0.003	0.22
55.9	57.5	1.6	1.5	93	103315	4E0	50	4.98	4.23	1.43	2.80	0.66	32.0	31.0	0.45	32.10	0.60	31.50	4.39	0.04	0.004	0.07
57.5	58.8	1.3	1.3	100	103316	4G8	60	4.83	6.39	2.22	4.17	0.65	43.0	42.0	0.21	19.20	1.40	17.80	23.16	0.02	0.003	0.11
58.8	60.4	1.6	1.5	93	103317	4G8	60	4.5	13.14	5.72	7.42	0.56	91.0	81.0	0.27	15.90	2.60	13.30	24.02	0.06	0.003	0.55
60.4	62.1	1.7	1.7	100	103318	4G8	60	4.2	11.15	4.22	6.93	0.62	70.0	64.0	0.34	12.50	1.90	10.60	24.87	0.06	0.005	0.41
62.1	63.0	0.9	0.9	99	103319	4L1	120	2.95	1.17	0.57	0.60	0.51	10.0	10.0	0.21	5.30	3.60	1.70	8.83	0.05	0.004	0.4
63.0	64.8	1.8	1.8	99	103320	4E8	50	4.7	2.66	1.32	1.34	0.50	21.0	21.0	0.93	33.00	6.90	26.10	0.44	0.33	0.003	0.84
64.8	66.4	1.6	1.6	100	103321	4C0	30	4.53	0.60	0.24	0.36	0.60	19.0	18.0	1.20	31.40	2.50	28.90	0.65	0.28	0.005	0.26
66.4	68.0	1.6	1.5	93	103322	4C0	30	4.26	0.29	0.16	0.13	0.45	11.0	11.0	1.06	30.80	2.60	28.20	0.08	0.32	0.002	0.21
68.0	69.8	1.8	1.8	99	103323	4C0	30	3.73	0.53	0.39	0.14	0.26	14.0	13.0	0.72	26.20	2.70	23.50	0.11	0.41	0.005	0.12
69.8	71.6	1.8	1.8	100	103324	4C0	30	3.53	0.35	0.21	0.14	0.40	10.0	11.0	1.27	25.70	2.30	23.40	0.18	0.22	0.004	0.18
71.6	73.5	1.9	1.8	94	103325	4C0	30	3.71	1.15	0.49	0.66	0.57	4.0	6.0	2.37	25.30	4.00	21.30	0.08	0.41	0.002	0.13
73.5	75.3	1.8	1.8	99	103326	4C0	30	3.68	0.34	0.20	0.14	0.41	2.0	2.0	1.20	26.90	4.06	22.84	0.02	0.26	0.005	0.14
75.3	77.1	1.8	1.8	100	103327	4C0	30	3.89	12.11	11.54	0.57	0.05	100.0	90.0	1.47	19.90	2.20	17.70	0.09	0.34	0.002	0.1

From (ft)	To (ft)	Intvl (ft)	Recov (ft)	Recov (%)	Sample No	Lithology	Rock Code (numeric)	SG pulp	Pb+Zn (%)	Pb (%)	Zn (%)	Zn/ (Pb+Zn)	Ag-AA (g/t)	Ag-FA (g/t)	Au (g/t)	Po+Py (%)	Po (Sol Fe) (%)	Py (Insol Fe) (%)	BaO (%)	Cu (%)	Hg (%)	Mn (%)
77.1	78.0	0.9	0.9	99	103328	4C0	30	3.89	25.11	23.23	1.88	0.07	224.0	204.0	4.49	14.70	1.80	12.90	0.02	0.19	0.003	0.12
78.0	79.9	1.9	1.8	94	103329	4C0	30	3.63	3.68	2.88	0.80	0.22	25.0	24.0	2.06	22.20	2.64	19.56	0.06	0.58	0.002	0.13
79.9	81.7	1.8	1.8	100	103330	4C8	30	3.62	1.97	0.77	1.20	0.61	7.0	10.0	0.65	26.90	15.30	11.60	0.02	0.21	0.002	1.9
81.7	82.9	1.2	1.2	99	103331	4C8	30	3.65	0.77	0.56	0.21	0.27	8.0	13.0	0.31	23.60	5.70	17.90	0.13	0.28	0.008	0.55
82.9	84.7	1.8	1.8	100	103332	4C8	30	3.46	0.97	0.52	0.45	0.46	2.0	6.0	0.27	20.10	5.50	14.60	0.10	0.05	0.004	0.57
84.7	86.1	1.4	1.4	99	103333	4C8	30	3.28	4.25	1.44	2.81	0.66	10.0	15.0	0.55	19.60	10.50	9.10	0.12	0.06	0.002	1.02
86.1	87.8	1.7	1.7	99	103293	4D07	80	3.59	12.31	3.30	9.01	0.73	50.0	-1	0.62	21.50	5.60	15.90	0.11	0.13	0.002	0.54
87.8	89.6	1.8	1.8	100	103294	4C0	30	3.03	6.55	2.98	3.57	0.55	51.0	-1	0.96	10.50	2.10	8.40	0.18	0.05	0.002	0.09
89.6	91.4	1.8	1.8	99	103295	4C0	30	3.39	2.13	0.81	1.32	0.62	13.0	-1	0.86	23.60	6.90	16.70	0.04	0.31	0.002	0.68
91.4	93.3	1.9	1.8	94	103296	4C0	30	3.27	1.36	0.43	0.93	0.68	10.0	-1	0.75	19.60	4.20	15.40	0.07	0.19	0.002	0.19
93.3	95.1	1.8	1.8	100	103297	4L0	120	-1	-1	-1	-1	0	-1	-1	0.01	-1	-1	-1	-1	0.06	-1	-1
95.1	96.9	1.8	1.8	99	103298	4L0	120	-1	-1	-1	-1	0	-1	-1	0.01	-1	-1	-1	-1	0.13	-1	-1
96.9	98.8	1.9	1.8	94	103299	4L0	120	-1	-1	-1	-1	0	-1	-1	0.55	-1	-1	-1	-1	0.16	-1	-1
98.8	100.3	1.5	1.5	100	103300	4L0	120	-1	-1	-1	-1	0	-1	-1	0.14	-1	-1	-1	-1	0.39	-1	-1
100.3	101.8	1.5	1.5	100	103351	4L0	120	-1	-1	-1	-1	0	-1	-1	0.34	-1	-1	-1	-1	0.27	-1	-1
101.8	103.0	1.2	1.2	100	103352	4L0	120	-1	-1	-1	-1	0	-1	-1	0.01	-1	-1	-1	-1	0.07	-1	-1
103.0	117.0	14.0	-1	-1	0	WASTE	0	-1	-1	-1	-1	0	-1	-1	-1	-1	-1	-1	-1	-1	-1	-1
117.0	118.9	1.9	1.8	94	103353	4L0	120	-1	-1	-1	-1	0	-1	-1	0.01	-1	-1	-1	-1	0.04	-1	-1
118.9	120.7	1.8	1.8	100	103354	4L0	120	-1	-1	-1	-1	0	-1	-1	0.01	-1	-1	-1	-1	0.01	-1	-1
120.7	122.5	1.8	1.8	99	103355	4L0	120	-1	-1	-1	-1	0	-1	-1	0.55	-1	-1	-1	-1	0.01	-1	-1
122.5	124.4	1.9	1.8	94	103356	4L0	120	-1	-1	-1	-1	0	-1	-1	0.69	-1	-1	-1	-1	0.01	-1	-1
124.4	126.2	1.8	1.8	100	103357	4L0	120	-1	-1	-1	-1	0	-1	-1	0.01	-1	-1	-1	-1	0.12	-1	-1
126.2	128.0	1.8	1.8	99	103358	4L0	120	-1	-1	-1	-1	0	-1	-1	0.01	-1	-1	-1	-1	0.05	-1	-1
128.0	129.8	1.8	1.7	94	103359	4L0	120	-1	-1	-1	-1	0	-1	-1	0.01	-1	-1	-1	-1	0.09	-1	-1
129.8	131.7	1.9	1.8	94	103360	4L0	120	-1	-1	-1	-1	0	-1	-1	0.01	-1	-1	-1	-1	0.13	-1	-1
131.7	133.5	1.8	1.8	99	103361	4L0	120	-1	-1	-1	-1	0	-1	-1	0.01	-1	-1	-1	-1	0.41	-1	-1
133.5	135.3	1.8	1.8	99	103362	4L0	120	-1	-1	-1	-1	0	-1	-1	0.01	-1	-1	-1	-1	0.34	-1	-1
135.3	137.2	1.9	1.8	94	103363	4L0	120	-1	-1	-1	-1	0	-1	-1	0.01	-1	-1	-1	-1	0.37	-1	-1
137.2	139.6	2.4	2.4	99	103364	4L0	120	-1	-1	-1	-1	0	-1	-1	0.01	-1	-1	-1	-1	0.10	-1	-1
139.6	176.8	37.2	-1	-1	0	WASTE	0	-1	-1	-1	-1	0	-1	-1	-1	-1	-1	-1	-1	-1	-1	-1

Page 1 of 7

CYPRUS ANVIL MINING CORPORATION

DIAMOND DRILL CORE LOG

Hole Number: V-47-R

Project: VANGORDA

Location: VANGORDA PLATEAU

Claim: _____

Terr. Plane Co-ords.: _____ N

_____ E

Grid Co-ords.: _____

_____

Elevation: _____

Total Depth: 580.0

Fabric Orientation Diagram:

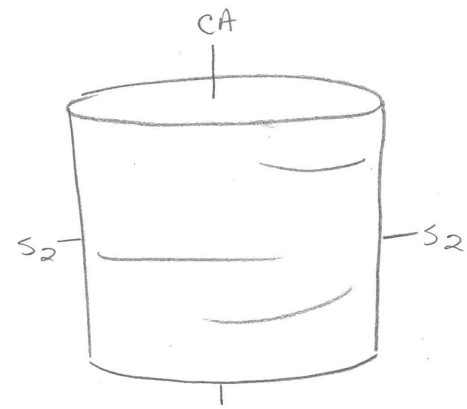

All symmetry determinations looking

NW with S2 dipping

SW with dip azimuth 220.

Purpose: _____

Logged by: JWM Date(s) Logged: _____

Drilling Contractor: A.D.D.

Core: Size From To Collar Cased and Capped: ____

_____ _____ _____

_____ _____ _____

_____ _____ _____

Started: _____ Completed: _____

Cyprus Anvil Mining Corp. Page 2 of 7

Diamond Drill Core Log

DDH V-47-R

Code	Drillhole	Elevation	Northing	Easting	Comments
1	2 8	10 16	17 24	25 32	34 48
T	V-47-R	1149.89	9031301.9	594053.4	FEET

Code	Drillhole	Depth	Zenith Angle	True Azimuth	Comments
1	2 8	10 14	22 26	28 32	34 56
R	V-47-R	0 0	1810.0		AT COLLAR
R	V-47-R	1612 0	1781.0	0938.0	
R	V-47-R	2162 0	1781.2	0943.0	
R	V-47-R	3335 0	1781.0	0933.0	GYRO SURVEY
R	V-47-R	3620 0	1771.2	0733.0	ACID ZEM = 1778° @ 3381'
R	V-47-R	4620 0	1721.2	0983.0	ACID ZEM = 1716° @ 4481'
R	V-47-R	5620 0	1701.8	0983.0	ACID ZEM = 1722° @ 5481'
R					
R					
R					
R					
R					
R					
R					
R					
R					

Code	Drillhole	Comments, Errant Remarks, Snivellings and /or Lewd Suggestions
1	2 8	10 47

DDH V-47-R (2 8) Cyprus Anvil Mining Corp. Lithologic Log Page 3 of 7 Logged By: JWM

Code	From	To	Unit	Code	Description
1	10 14	16 20	22 23	25 27	
L	1100	11106	01		TRICONED NO CORE
L	11100	11330	02	4A10	Pb+Zn ≈ 4% overall, very graphitic
L	11330	11380	02	4GP	Fine grained, locally 4FL
L	11380	11415	03	4EEK	50, 40, 10, minor baritic facies
L	11415	11440	04	4EK	50/50
L	11440	11500	05	4G8	mush mash of 460+468 where 468 occurs 46 is coarse grained.
L	11500	11580	06	4K37	Variably calc.
L	11580	11608	07	4G8	med. grained.
L	11608	11641	08	4L10	0.5' 50 2 Rk. at beginning of interval.
L	11641	11705	09	4E0	→4E8
L	11705	11785	10	4G8	Coarse grained Variant
L	11785	11814	11	5D16	
L	11814	11885	12	4E0	→ 4E8
L	11885	12038	13	4G8	Variably calcareous throughout
					~~Eg~~ Eg. Variant of 46 with Fe2O3
L	12038	12067	14	4L1	20% carbonates - fizzes in 10%
					20% silica.
L	12067	12125	15	4E8	
L	12125	12260	16	4C0	→4CE, ≈ 70-80% FeS, minor magnetite. + minor Po
L	12260	12553	17	4C0	≈ 20-50% py,
					0-5% po, minor mag.
					Variable cpy - overall quite low
					Variable base metal overall " "
					in areas approaches "46 texture"
L	12553	12612	18	4C10	as above but Variably calcareous
L	12612	12820	19	4C8	Variable base metals → 4D8
L	12820	12825	20	5D10	Calcareous
L	12825	12880	21	4D07	
L	12880	13056	22	4C10	→ 4C8 Variable Fe2O3 locally
					to 4D, Variable Cu content, locally
					to 4C9
L	13056	13146	23	4L10	
L	13146	13380	24	4L10	→ 4L9, Variably calc. throughout
					carbonates as distinct laminations +
					horizons within 4L split for Cu, Au

DDH V-47-R (2 / 8)

Cyprus Anvil Mining Corp.

Lithologic Log

Page 4 of 7

Logged By: JWM

Code	From	To	Unit	Code	Description
1	10 14	16 20	22 23	25 27	
L	13380	13500	25	4K10	→ 4L6 minor carbonates
L	13500	13700	26	5B12	musc >> chlorite (musc+chl = 5%?)
L	13700	13840	27	4L13	calcareous.
L	13840	14180	28	4L67	Variably calcareous throughout.
L	14190	14485	29	4L76	91 split for Cu, Au
L	14485	14580	30	4L41	796 " " " "
L	14580	14880	31	5B619	locally → 4L6
L	14880	15080	32	4L67	Variably calcareous
L	15080	15137	33	4L13	
L	15137	15148	34		fault gouge
L	15148	15280	35	4L40	
L	15280	15320	36	4A10	
L	15320	15360	37	4K10	
L	15360	15480	38		in + out of fault zone
					60-70% fault gouge
					40-30% SDG 2 Rk.
					difficult if not useless to
					determine lith breaks within
					this zone.

DDH V-47-R (2 8) Cyprus Anvil Mining Corp. Page 5 of 7

Structural Log Logged By: JWM

Code	From	To	Feature	Sym	S_1 Dip	S_1 Direct.	S_2 Dip	S_2 Direct.	Description
1	10 14	16 20	22 24	26	28	32	34	38	
S		1112.0	PS2				20	210	
S		1119.0	PS2				35	210	
S		1133.0	PS2	Z			60	210	
S		1148.0	S2				70	210	
S		1168.0	S2				73	210	
S		1178.0	S2				70	210	
S		1198.0	S2				75	210	
S		1210.8.0	S2				83	210	
S		1236.0	S2				70	210	
S		1258.0	S2				75	210	
S		1278.0	S2				80	210	
S		1298.0	S2				80	210	
S		1306.0	S2				80	210	R region 133-306
									SJI Fold + AL
S		1316.4	GS2	S			80	210	
S		1318.0	GS2	Z					Z region 316.4 - 318.0
S		1331.3	GS2	M			75	210	
S		1348.0	GS2				80	210	
S		1358.0	GS2				70	210	
S		1368.0	GS2				70	210	
S		1380.0	GS2				80	210	
S		1397.0	GS2	S					S region 1348.0 - 1397.0
S		1408.0	GS2	M			80	210	
S		1428.0	GS2	S			53	210	408 - 428 S region
S		1448.0	PS2				80	210	
S		1458.0	PS2				65	210	
S		1468.0	PS2				64	210	
S		1487.0	PS2				70	210	
S		1498.0	PS2	P			85	210	No symm observed.
S		1501.7.0	PS2	S			70	210	
S		1521.8.0	PS2				50	210	
S		1536.0	S2				60	210	536 - 580 broken + rippled
									core, where S2 is observable
									attitudes very wobbly

DDH V-47-R (2 8)

Cyprus Anvil Mining Corp.

Geochemical Log (Sampler's Copy)

Page 6 of 7
Logged By: IWM
Sampled By:

Code	From	To	Sample No.	Description		
1	10 14	16 20	22 27	UNIT	LENGTH	REC.
P	1/110 6	1/150	V1 13199	4A0	4.4	4.1
P	1/150	1/210 0	V1 32010	4A0	5.0	5.0
P	1/210 0	1/250	V1 33101	4A0	5.0	5.0
P	1/250	1/310 0	V1 33102	4A0	5.0	5.0
P	1/310 0	1/330	V1 33103	4A0	3.0	3.0
P	1/330	1/380	V1 33104	4G0	5.0	5.0
P	1/380	1/430	V1 33105	4EFK	5.0	5.0
P	1/430	1/480	V1 33106	4G8/E	5.0	5.0
P	1/480	1/500	V1 33107	4G8	2.0	2.0
P	1/500	1/580	V1 33108	4L37	8.0	8.0
P	1/580	1/608	V1 33109	4G8	2.8	2.8
P	1/608	1/641	V1 33110	4L0	3.3	3.3
P	1/641	1/705	V1 33111	4E0	6.4	6.4
P	1/705	1/745	V1 33112	4G8	4.0	4.0
P	1/745	1/785	V1 33113	4G8	4.0	4.0
P	1/785	1/835	V1 33114	4E/5D	5.0	5.0
P	1/835	1/885	V1 33115	4E0	5.0	5.0
P	1/885	1/930	V1 33116	4G8	4.5	4.5
P	1/930	1/980	V1 33117	4G8	5.0	5.0
P	1/980	2038	V1 33118	4G8	5.8	5.8
P	2038	2067	V1 33119	4L1	2.9	2.9
P	2067	2125	V1 33120	4E8	5.8	5.8
P	2125	2180	V1 33121	4C0	5.5	5.5
P	2180	2230	V1 33122	4C0	5.0	5.0
P	2230	2290	V1 33123	4C0	6.0	6.0
P	2290	2350	V1 33124	4C0	6.0	6.0
P	2350	2410	V1 33125	4C0	6.0	6.0
P	2410	2470	V1 33126	4C0	6.0	6.0
P	2470	2530	V1 33127	4C0	6.0	6.0
P	2530	2560	V1 33128	4C0	3.0	3.0
P	2560	2620	V1 33129	4C0	6.0	6.0
P	2620	2680	V1 33130	4C8	6.0	6.0
P	2680	2720	V1 33131	4C8	4.0	4.0
P	2720	2780	V1 33132	4C8	6.0	6.0
P	2780	2825	V1 33133	4C8	4.5	4.5

DDH VI-A7-R (2 / 8)

Cyprus Anvil Mining Corp.

Geochemical Log (Sampler's Copy)

Page 7 of 7

Logged By: _____

Sampled By: _____

Code	From	To	Sample No.	Description			
1	10 14	16 20	22 27	UNIT	LENGTH	REC.	
P	12812 5	12818 0	VI 32193	4007	5.5	5.5	
P	12818 0	12940	VI 32194	4CO	6.0	6.0	
P	12940	13000	VI 32195	4CO	6.0	6.0	
P	13000	13060	VI 32196	4CO	6.0	6.0	
P	13060	31120	VI 32197	4LO	6.0	6.0	Cu, Au only
P	31120	31180	VI 32198	4LO	6.0	6.0	" " "
P	31180	32400	VI 32199	4LO	6.0	6.0	" " "
P	32400	32900	VI 33000	4LO	5.0	5.0	" " "
P	32900	33400	VI 33351	4LO	5.0	5.0	" " "
P	33400	33800	VI 33352	4LO	4.0	4.0	" " "
P	31840	33900	VI 33353	4LO	6.0	6.0	Cu, Au only
P	33900	39160	VI 33354	4LO	6.0	6.0	" " "
P	39160	A1020	VI 33355	4LO	6.0	6.0	" " "
P	A1020	A1080	VI 33356	4LO	6.0	6.0	" " "
P	A1080	A1140	VI 33357	4LO	6.0	6.0	" " "
P	A1140	A1200	VI 33358	4LO	6.0	5.8	" " "
P	A1200	A1260	VI 33359	4LO	6.0	5.6	" " "
P	A1260	A3120	VI 33360	4LO	6.0	6.0	" " "
P	A3120	A3180	VI 33361	4LO	6.0	6.0	" " "
P	A3180	A4440	VI 33362	4LO	6.0	6.0	" " "
P	A4440	A5100	VI 33363	4LO	6.0	6.0	" " "
P	A5100	A5180	VI 3364	4LO	8.0	8.0	" " "

000560

TABLE 1
ANVIL DISTRICT
DETAILED LOGGING LITHOSTRATIGRAPHIC CODE
MAIN DEPOSIT AREA

Unconsolidated Overburden				
Unit 11		11	A	Triconed, no recovery
		11	B	Till, silt, sand - all unconsolidated
Intrusive Rocks				
Unit 10	928	10	AB	Granite - Anvil Batholith
				$10AB_{mm}$ Mt. Mye phase biotite-muscovite
				$10AB_{o}$ Orchay phase biotite-hornblende
				$10AB_{m}$ Majorie phase biotite-hornblende
	939	10	C	Pegmatite
	934	10	E	Biotite-hornblende granite porphyry
	925	10	F	Smokey quartz-feldspar porphyry
	938	10	Q	Bull qtz veins/pods
				1 Foliated/lineated
				2 Porphyritic
				3 Aphanitic
				4 Smokey qtz-bearing
				5 Muscovite-bearing
				6 Kspar-bearing
				7 Biotite-bearing
				8 Amphibole-bearing
				9 Altered (kaolinite, montmorillonite)
				0 Normal (equigranular)
Vangorda Formation				
Unit 5	936	5	A	Variably calcareous, graphitic phyllite (= 1E, hosts Units 2/4)
		5	A*	Graphitic fault rock with shear band fabric and vein quartz, altered metabasite clasts
	920		B	Calcareous muscovite-chlorite+/- biotite phyllite (greenschist equivalent of 3D)
	908		C	Metabasite (includes pyroxenite)
	910		D	Chloritic phyllite (also logged as 5F locally)
	904		E	Phyllitic marble and silicated marble
	949		G	Variably calcareous, graphitic phyllite (above basal graphitic unit)
				1 Siliceous
				2 Carbonaceous
				3 Calcareous
				4 Altered, pyritic (white mica envelope)
				5 Banded/laminated
				6 Non-calcareous
				7 Chlorite laminations
				8 Chloritic
				9 Sulfide-bearing
				0 Normal
				* Carbonate-bearing

Vangorda Formation				
Unit 3	913	3	D	Calc-silicate phyllite/schist (amphibolite facies equivalent of 5B)
Faro, Grum, Vangorda, DY Deposits Conformable Contact				
Unit 2/4	922	2/4	A	Sulfide-bearing, ribbon-banded, graphitic quartzite
	915		B	Pyrite-free quartzite (may contain base metal sulfides)
	916		C	Base metal-poor, pyritic quartzite
	942		D	Base metal-bearing, pyritic quartzite
	918		E	Massive pyritic sulfides
	923		F	Buckshot facies, massive pyritic sulfides
	928		G	Baritic facies, massive sulfides/sulfates (>10% BaS04)
	924		H	Pyrrhotitic facies, massive sulfides
	949		J	Non-pyritic, massive sulfides/oxides (vein type sulfides)
	921		K	Dolomite-bearing, massive pyritic sulfides
				1 Siliceous
				2 Fine pyrite/marcasite-bearing
				3 Coarse, porphyroblastic pyrite-bearing
				4 Sphalerite and/or galena-bearing
				5 Carbonaceous
				6 Barite-bearing
				7 Pyrrhotite-bearing
				8 Magnetite-bearing
				9 Chalcopyrite-bearing
				0 Normal
				* Carbonate-bearing
Alteration Facies for Metapelite Units				
Unit 2/4L				White muscovite>qtz-chl-bio-phyllite (generally sulfide-bearing)
				1 Siliceous
				2 Pyrite-bearing
				3 Talc/kaolinite-bearing
				4 ZnS and/or PbS-bearing
				5 Carbonate-bearing
				6 Chl-bio>qtz-musc phyllite
				7 Pyrrhotite-bearing
				8 Magnetite-bearing
				9 Chalcopyrite-bearing
				0 Normal
Mt. Mye Formation (Greenschist Facies)				
Unit 3	916		3-I	Graphitic quartzite in non-calcareous phyllite/schist
	941		G	Non-calcareous muscovite-chlorite+/biotite phyllite/schist (= 1C, 1D)
	906		F	Marble and silicated marble (=1G)
	963		E	Graphitic phyllite/schist (= 5A)
	913		D	Calc-silicate phyllite/schist

	908	C	Metabasite (includes pyroxenite)
	946	B	Chloritic phyllite/schist (c.f. 5D)
	912	3-A	Transition zone with Unit 1 (interbanded chloritic phyllite, graphitic phyllite, and pelites of Vangorda and Mt. Mye Fms.)
		1	Siliceous
		2	Non-calcareous
		3	Calcareous
		4	Altered, pyritic (wme)*
		5	Banded/laminated
		6	Sulfide-bearing
		7	Chlorite laminations
		8	Chloritic
		9	Carbonaceous
		0	Normal

Mt. Mye Formation (Amphibolite Facies)

Unit 1	902	1-B	Tactite and silicated marble (=3F)
	943	C	Quartzo-feldspathic, biotite-muscovite gneiss/schist (= 3G)
	947	D	Carbonaceous biotite-muscovite-andalusite schist (= 3G)
		1CD	Biotite-muscovite-andalusite schist (= 3G) transitional between 1C and 1D
	967	E	Graphitic schist (=5A)
	908	F	Metabasite (=3C), chloritic schist/amphibolite
	901	G	Marble and silicated marble (= 3F)
	910	1-H	Chloritic schist (c.f. 5D)
		1	Siliceous
		2	Carbonaceous
		3	Calcareous
		4	Altered, pyritic (wme)*
		5	Banded
		6	Clotted
		7	Staurolitic
		8	Chloritic
		9	Sulfide-bearing
		0	Normal

*(wme) White mica envelope

Carbonates
* carbonate
# calcite
$ dolomite
@ ankerite

pigage\lithocod
March 9, 1990

TABLE 1 ANVIL DISTRICT DETAILED LOGGING LITHOSTRATIGRAPHIC CODE

MAIN DEPOSIT AREA

LITHOSTRATIGRAPHIC CODE

Intrusive Rocks

Unit 10	928	10-A	Granodiorite (kspar>plag, quartz>10%)
	929	B	Adamellite (qtz monzonite)
	939	C	Pegmatite
	956	D	Quartz diorite (kspar<<plag, qtz>10%)
	934	E	Diorite (kspar<<plag, qtz 10)
	925	F	Monzonite (kspar>plag, qtz-10.)
	932	G	Pyroxenite
	937	H	Granite (kspar>plag, qtz>10%)
	930	I	Syenite (kspar>plag, qtz-10:)
	938	Q	Bull qtz veins/pods

1 Foliated/lineated
2 Porphyritic
3 Aphanitic
4 Smokey qtz-bearing
5 Muscovite-bearing
6 Kspar-bearing
7 Biotite-bearing
8 Amphibole-bearing
9 Altered (kaolinite, montmorillonite)
0 Normal (equigranular)

Carbonates

* carbonate
# calcite
$ dolomite
@ ankerite

Yangorda Formation — Intrusive Contact

Unit 5	936	5-A	Variably calcareous, graphitic phyllite (hosts Unit 4; ; 1E, hosts Unit 2)
	920	B	Calcareous muscovite-chlorite:biotite phyllite (greenschist equivalent of 3D)
	908	C	Metabasite
	910	D	Chloritic phyllite
	904	E	Phyllitic marble and silicated marble
	910	F	Laminarly banded, variably calcareous, chloritic phyllite (associated with 5C)
	949	G	Variably calcareous, graphitic phyllite.

1 Siliceous
2 Carbonaceous
3 Calcareous
4 Altered, pyritic (white mica envelope)
5 Banded/laminated
6 Non-calcareous
7 Chlorite laminations
8 Chloritic
9 Sulfide-bearing
0 Normal
* Carbonate-bearing

Faro, Grum, Yangorda, Or Deposits — Conformable Contact

Unit 2/4	922	2/4-A	Sulfide-bearing, ribbon-banded, graphitic quartzite
	915	B	Pyrite-free quartzite (may contain base metal sulfides)
	916	C	Base metal-poor, pyritic quartzite
	942	D	Base metal-bearing, pyritic quartzite
	918	E	Massive pyritic sulfides
	923	F	Buckshot facies, massive sulfides
	928	G	Baritic facies, massive sulfides/sulfates (>10%:$BaSO_4$)
	924	H	Pyrrhotitic facies, massive sulfides
	949	J	Non-pyritic, massive sulfides/oxides
	921	K	Carbonate-bearing, massive pyritic sulfides
	914	L	

1 Siliceous
2 Coarse, porphyroblastic pyrite-bearing
3 Fine pyrite/marcasite-bearing
4 Sphalerite and/or galena-bearing
5 Carbonaceous
6 Barite-bearing
7 Pyrrhotite-bearing
8 Magnetite-bearing
9 Chalcopyrite-bearing
0 Normal
* Carbonate-bearing

2/4L Muscovite-qtz-chl-bio-phyllite (generally sulfide-bearing)

1 Siliceous
2 Pyrite-bearing
3 Talc/kaolinite-bearing
4 ZnS and/or PbS-bearing
5 Carbonate-bearing
6 Chl-bio-qtz-musc phyllite
7 Pyrrhotite-bearing
8 Magnetite-bearing
9 Chalcopyrite-bearing
0 Normal

Mt. Mye Formation — Conformable Contact

Unit 3	916	3-1	Graphitic quartzite in non-calcareous phyllite/schist
	913	H	Tuffaceous calc-silicate phyllite/schist (assoc. with 3D; identical to 5F1
	941	G	Non-calcareous muscovite-chlorite:biotite phyllite/schist (; 1C, 1D)
	906	F	Marble and silicated marble (; 1G)
	963	E	Graphitic phyllite/schist (/ 5A)
	913	D	Calc-silicate phyllite/schist (u. greenschist to amphibolite facies equiv. of 5B)
	908	C	Metabasite
	946	B	Chloritic phyllite/schist (c.f. 5D)
	912	3-A	Transition zone with unit 1 (interbanded chloritic phyllite, graphitic phyllite and pelites of Yangorda and Mt. Mye Fms.)
	902	1-B	Tactite and silicated marble (/ 3F)
	943	C	Quartzo-feldspathic, biotite-muscovite gneiss/schist (; 3G)
	947	D	Carbonaceous biotite-muscovite-andalusite schist (; 3G)
	967	E	Graphitic schist (; 5A)
	908	F	Metabasite (; 3C)
	901	G	Marble and silicated marble (; 3F)
Unit 1	910	1-H	Chloritic schist (c.f. 5D)

1 Siliceous
2 Non-calcareous
3 Calcareous
4 Altered, pyritic (wme)*
5 Banded/laminated
6 Sulfide-bearing
7 Chlorite laminations
8 Chloritic
9 Carbonaceous
0 Normal

1 Siliceous
2 Carbonaceous
3 Calcareous
4 Altered, pyritic (wme)*
5 Banded
6 Clotted
7 Staurolitic
8 Chloritic
9 Sulfide-bearing
0 Normal

*(wme) White mica envelope

ANVIL STOP 1 (NORTHEAST OF VANGORDA PIT)

We are standing on the edge of the old exploration road on the Vangorda Plateau. Noncalcareous phyllite of the Mount Mye formation (Gull Lake Formation) outcrops along the edge of the road. This particular roadside exposure is in the footwall of the Vangorda deposit. Phyllite is in the muscovite-chlorite zone of the greenschist metamorphic facies.

The mountains just uphill to the northeast are cored by muscovite-biotite granite of the Anvil batholith. Monazite analyses from this granite yielded U-Pb dates of 109.3 ± 1.2 Ma and 103.9 ± 1.5 Ma. The contact between the granite and schists is the extensional Tie fault. Adjacent to the fault the granite contains S-C banding and the phyllite contains shear banding. S-C bands and shear bands consistently indicate south side down for the faulting.

The dominant foliation in our outcrop is the phase 2 axial planar crenulation cleavage. Phase 1 foliation occurs as microlithons in thin section. Phase 1 folds are northeast verging. Phase 2 folds are southwest verging. Minor folds plunge gently to the southeast and northwest. Phase 2 cleavage is undulating and dips gently southwest and northeast.

ANVIL STOP 2 (NORTHEAST PIT WALL OF VANGORDA DEPOSIT)

The Vangorda pit was mined during the interval 1990-1993. Waste dumps were placed immediately southwest (downstream) from the open pit. Ore was transported to the mill facility at the Faro minesite for processing.

The Vangorda diversion ditch exposes the carbonaceous phyllite of the basal part of the Vangorda formation. The Vangorda formation is juxtaposed against the host Mount Mye phyllite by the Northwest and Creek faults.

ANVIL STOP 3 (NORTHWEST PIT WALL OF GRUM DEPOSIT)

Pits walls in this immediate area consist of Vangorda formation calcareous phyllite. Interlaced with the calcareous phyllite are numerous basaltic dikes and sills. Basaltic rocks have same chemistry as the overlying Menzie Creek formation and are considered to be subvolcanic equivalents.

Rock samples and wall samples show a well-developed S2 crenulation cleavage. S2 is the dominant fabric in the phyllite and dips gently to the southwest or northeast.

In the pit wall a large variation in depth of overburden is visible. Northeast wall contains extensive glacial deposits. During the last glaciation the ice infilled a pre-existing stream valley with glacial material.

A vertical cross section through the Grum deposit displays an interference pattern between a large northeast verging phase 1 fold and a superimposed southwest verging phase 2 fold.

ANVIL STOP 4 (ORE TRANSFER PAD NORTH OF GRUM PIT)

Curragh Resources and Anvil Range Mining used this flat area as a staging area to transfer ore from the large pit trucks to smaller haul tracks. Ore was then trucked the 13 km along the haul road to the Faro millsite. Here you can find examples of the different ore quartzose, sulphide, and baritic ore types. Feel free to take photos and collect hand samples.

ANVIL STOP 5 (UPPER PIT WALL OF FARO DEPOSIT)

We will be walking along this bench in a general northerly direction. The walk will start in Vangorda fm calc-silicate rock. Farther along it will transition to graphitic schists of the basal Vangorda fm and then the biotite-andalusite schists of the Mt Mye fm. The bench will end with a pyrrhotite rich facies of the Faro orebody which has been intruded by biotite granodiorite of the Tay River plutonic suite (95.6 ± 1.0 Ma: $^{40}Ar/^{39}Ar$ on biotite).

As with the stops on the Vangorda Plateau, the dominant foliation here is the phase 2 crenulation cleavage. Faro deposit can be considered an egg sandwich. Massive sulphides and baritic sulphides form egg between bread slices of quartzose ore. Alteration extensive muscovite. Ore lithologies locally are altered to pyrrhotite. In places large magnetite lenses denote desulphidation of the original sulphide mineralogy.

Pit wall across the pit consists of footwall Mount Mye schist. Because it dips into the pit, there has been mass movement and failure along that wall. This wall is much more competent for two reasons: calc-silicate is very hard lithology and dominant foliation dips into the pit wall.

REFERENCES

Abbott, J.G., Gordey, S.P., and Tempelman-Kluit, D.J., 1986. Setting of stratiform, sediment-hosted lead-zinc deposits in Yukon and northeastern British Columbia. *In:* Mineral Deposits of Northern Cordillera, J.A. Morin (ed.), Canadian Institute of Mining and Metallurgy, Special Paper 37, p. 1-18.

Brown, D., 1993. Deformation and metamorphism of the Vangorda Pb-Zn massive sulphide deposit, Yukon Territory, Canada. Unpublished PhD thesis, Royal Holloway, University of London, 209 p.

Brown, D., 1994. Low temperature, low pressure deformation and metamorphism of the Vangorda massive sulphide orebody, Yukon, Canada. Mineralium Deposita, vol. 29, p. 330-340.

Brown, D. and McClay, K., 1994. Structural geology of the Vangorda Pb-Zn-Ag orebody, Yukon, Canada. Ore Geology Reviews, vol. 9, p. 61-78.

Carne, R.C. and Cathro, R.J., 1982. Sedimentary exhalative (sedex) zinc-lead-silver deposits, northern Canadian Cordillera. Canadian Institute Mining Metallurgy Bulletin, vol. 75, no. 840, p. 66-78.

Casselman, S. (compiler), 2015. Yukon Mineral Deposits Summary 2015. Yukon Geological Survey, 28 p.

Chisholm, E.O., 1957. Gephysical exploration of a lead-zinc deposit in Yukon Territory. *In:* Methods and case histories in mining geophysics, Sixth Commonwealth Mining and Metallurgy Congress, p. 269-277.

Cobbett, R.N., 2014. Preliminary observations on the geology of the Anvil Lake area (parts of NTS 105K11 & 12) central Yukon. *In:* Yukon Exploration and Geology 2013, K.E. MacFarlane, M.G. Nordling, and P.J. sack (eds.), Yukon Geological Survey, p. 33-51.

Cobbett, R.N., 2015. Geological Map of the Anvil Lake area, Central Yukon, parts of NTS 105K11 & 12. Yukon Geological Survey, Open File 2015-2 (1:50 000 scale).

Cobbett, R.N., 2016. Preliminary observations on the geology of Tay Mountain Area (parts of NTS 105K/12 and 13, 105L09 and 16), central Yukon. *In:* Yukon Exploration and Geology 2015, K.E. MacFarlane and M.G. Nordling (eds.), Yukon Geological Survey, p. 79-98.

Cohen, K.M., Finney, S.C., Gibbard, P.L., and Fan, J.-X., 2013 (updated). The ICS international Chronostratigraphic chart. Episodes, v. 36, p. 199-204.

Colpron, M. and Nelson, J.L., 2011. A Digital Atlas of Terranes for the Northern Cordillera. Yukon Geological Survey and British Columbia Geological Survey. Downloaded from www.geology.gov.yk.ca/bedrock_terrane.html on February 1, 2016.

Colpron, M., Nelson, J.L., and Murphy, D.C., 2007. Northern Cordilleran terranes and their interactions through time. GSA Today, vol. 17, no. 4/5, p. 4-10.

Gabrielse, H., 1967. Tectonic evolution of the northern Canadian Cordillera. Canadian Journal of Earth Sciences, vol. 4, p. 271-298.

Gabrielse, H., Murphy, D.C. and Mortensen, J.K., 2006. Cretaceous and Cenozoic dextral orogeny-parallel displacements, magmatism, and paleogeography, north-central Canadian Cordillera. *In:* Paleogeography of the North American Cordillera: evidence for and against large-scale displacements, J.W. Haggart, R.J. Enkin and J.W.H. Monger (eds.), Geological Association of Canada, Special Paper 46, p. 255-276.

Gaffin, J., 1980. Cashing In. D.W. Friesen & Sons Ltd., 215 p.

Gordey, S.P., 1983. Thrust faults in the Anvil Range, and a new look at the Anvil Range Group, south-central Yukon Territory. Geological Survey of Canada, Paper 83-1A, p. 225-227.

Gordey, S.P., 2013. Evolution of the Selwyn Basin region, Sheldon Lake and Tay River map areas, central Yukon. Geological Survey of Canada, Bulletin 599, 176 p.

Gordey, S.P. and Anderson, R.G., 1993. Evolution of the northern Cordilleran miogeocline, Nahanni map area (105I), Yukon and Northwest Territories. Geological Survey of Canada, Memoir 428, 214 p.

Gordey, S.P. and Irwin, S.E.B., 1987. Geology, Sheldon Lake and Tay River map areas, Yukon Territory. Geological Survey of Canada, Map 19-1987 (3 sheets; 1:250000 scale).

Gustafson, L.B. and Williams, N., 1981. Sediment-hosted stratiform deposits of copper, lead, and zinc. Economic Geology, 75th Anniversary Volume, p. 139-178.

Jennings, D.S. and Jilson, G.A., 1986. Geology and sulphide deposits of Anvil Range, Yukon. *In:* Mineral Deposits of Northern Cordillera, J.A. Morin (ed.), Canadian Institute of Mining and Metallurgy, Special Volume 37, p. 319-361.

Meschede, M., 1986. A method of discriminating between different types of mid-ocean ridge basalts and continental tholeiites with the Nb-Zr-Y diagram. Chemical Geology, vol. 56, p. 207-218.

Modene, J.S., 1982. Origin and sulfur isotope geochemistry of the Grum deposit, Yukon Territory, Canada. Unpublished M.Sc. dissertation, University of Wisconsin, 158 p.

Mortensen, J.K. and Jilson, G.A., 1985. Evolution of the Yukon-Tanana Terrane: evidence from southeastern Yukon Territory. Geology, vol. 13, p. 806-810.

Mortensen, J.K., Hart, C.J.R., Murphy, D.C. and Heffernan, S., 2000. Temporal evolution of early and mid-Cretaceous magmatism in the Tintina Gold Belt. *In:* The Tintina Gold Belt: Concepts, Exploration, and Discoveries, T.L. Tucker and M.T. Smith (eds.), British Columbia and Yukon Chamber of Mines, Special Volume 2, p. 49-58.

Moynihan, D., 2014. Bedrock geology of NTS 106B/04, Eastern Rackla Belt. *In:* Yukon Exploration and Geology 2013, K.E. MacFarlane, M.G. Nordling, and P.J. Sack (eds.), Yukon Geological Survey, p. 147-167.

Pearce, J.A., 1996. A user's guide to basalt discrimination diagrams. *In:* Trace Element Geochemistry of Volcanic Rocks: Applications for Massive Sulphide Exploration, D.A. Wyman (ed.), Geological Association of Canada, Short Course Notes, vol. 12, p. 79-113.

Pigage, L.C., 1990. Anvil Pb-Zn-Ag district, Yukon Territory, Canada. *In:* Mineral Deposits of the Northern Canadian Cordillera, Yukon-Northeastern British Columbia, J.G. Abbott and R.J.W. Turner (eds.), Geological Survey of Canada, Open File 2169, p. 283-308.

Pigage, L.C., 2004. Bedrock geology compilation of the Anvil District (parts of NTS 105K/02, 3, 5, 6, 7 and 11), central Yukon. Yukon Geological Survey, Bulletin 15, 103 p.

Ramsay, J.G., 1967. Fold and fracturing of rocks. McGraw-Hill Book Company, New York, 568 p.

Roddick, J.A. and Green, L.H., 1961. Tay River, Yukon Territory. Geological Survey of Canada, Map 13-1961 (1:253,440 scale).

Shervais, J.W., 1982. Ti-V plots and the petrogenesis of modern and ophiolitic lavas. Earth and Planetary Science Letters, vol. 59, p. 101-118.

Smith, J.M. and Erdmer, P., 1990. The Anvil aureole, an atypical mid-Cretaceous culmination in the northern Canadian Cordillera. Canadian Journal of Earth Sciences, vol. 27, p. 344-356.

Sun, S.-S. and McDonough, W.F., 1989. Chemical and isotopic systematics of oceanic basalts: implications for mantle composition and processes. *In:* Magmatism in the Ocean Basins, A.D. Saunders and M.J. Norry (eds.), Geological Society Special Publication 42, p. 313-345.

Tempelman-Kluit, D., 1972. Geology and origin of the Faro, Vangorda, and Swim concordant zinc-lead deposits, central Yukon Territory. Geological Survey of Canada, Bulletin 208 (1:250 000 scale), 73 p.

Winchester, J.A. and Floyd, P.A., 1977. Geochemical discrimination of different magma series and their differentiation products using immobile elements. Chemical Geology, vol. 20, p. 325-343.

Wood, D.A., 1980. The application of a Th-Hf-Ta diagram to problems of tectonomagmatic classification and to establishing the nature of crustal contamination of basaltic lavas of the British Tertiary volcanic province. Earth and Planetary Science Letters, vol. 50, p. 11-30.

Faro Mine Complex
SED-EXhumed Field Trip
Remediation

GAC-MAC 2016
May 30-31
2016

Remediation Authors:
Esteban Larrea
Dustin Rainey

Faro Mine Complex (FMC): General Location

The FMC is located in sub-arctic, mountainous terrain of Yukon Territory at 62ºN latitude. It was operational from 1969 to 1998, when it was abandoned. In its day, the mine was one of the largest lead-zinc mines in the world. It is now the largest unfunded acid rock drainage contaminated mine site in Canada. The Faro Mine Remediation Project (FMRP) is jointly managed by Yukon Government and the Government of Canada (Indigenous and Northern Affairs Canada - INAC).

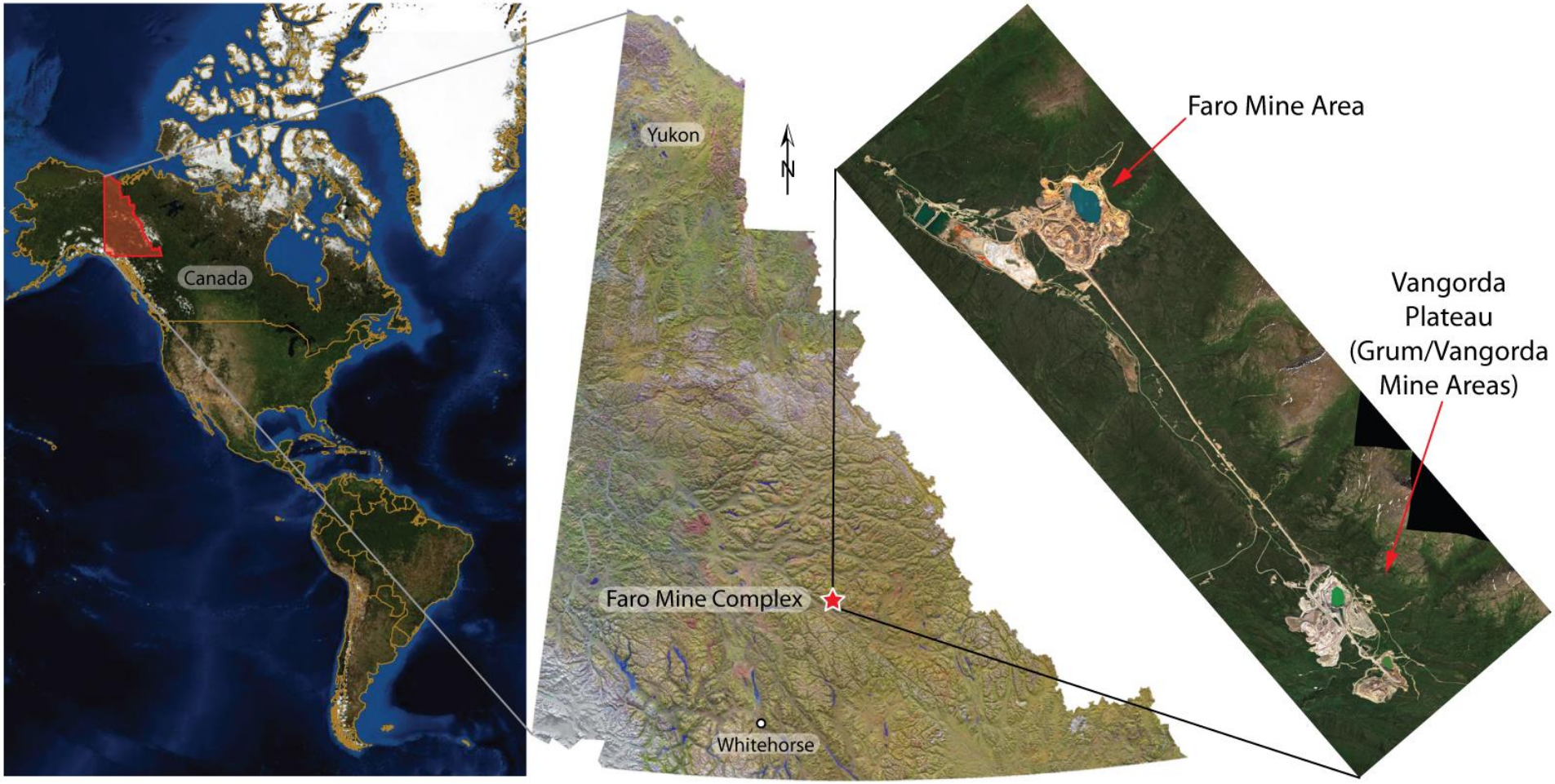

Acid Rock Drainage

Photo taken over the low-grade ore piles close to the Mill Area.

Acid Rock Drainage (ARD) is a term used to describe a set of chemical reactions. These reactions occur when sulphur-containing rock is exposed to water and oxygen.

When oxygen and water come into contact with reduced sulphur (sulphide) containing rock, acid is produced. This acid can dissolve metals from the surrounding rocks and release them into ground and surface waters. High levels of metals and acid can be harmful to fish and other aquatic life.

$$4FeS_2 + 15O_2 + 14H_2O \rightarrow 4Fe(OH)_3 + 8SO_4^{2-} + 16H^+$$

Acid Rock Drainage

Crushing of sulphide-containing rock during mining increases the amount of acid rock drainage produced because more rock surfaces are exposed to oxygen and water present in the atmosphere.

The processes that create acid rock drainage have begun at the Faro Mine Complex, and scientists predict that the amount of metals released will continue to increase for the next 400 to 800 years.

The presence of naturally-occurring bacteria called *Thiobacillus ferrooxidans* can greatly increase the rate of acid rock drainage reactions. The bacteria use sulphur and iron present in rocks as a source of energy and, under the right conditions, can accelerate the rate of acid rock drainage production. The *Thiobacillus ferrooxidans* bacteria is present and active at the Faro Mine Complex.

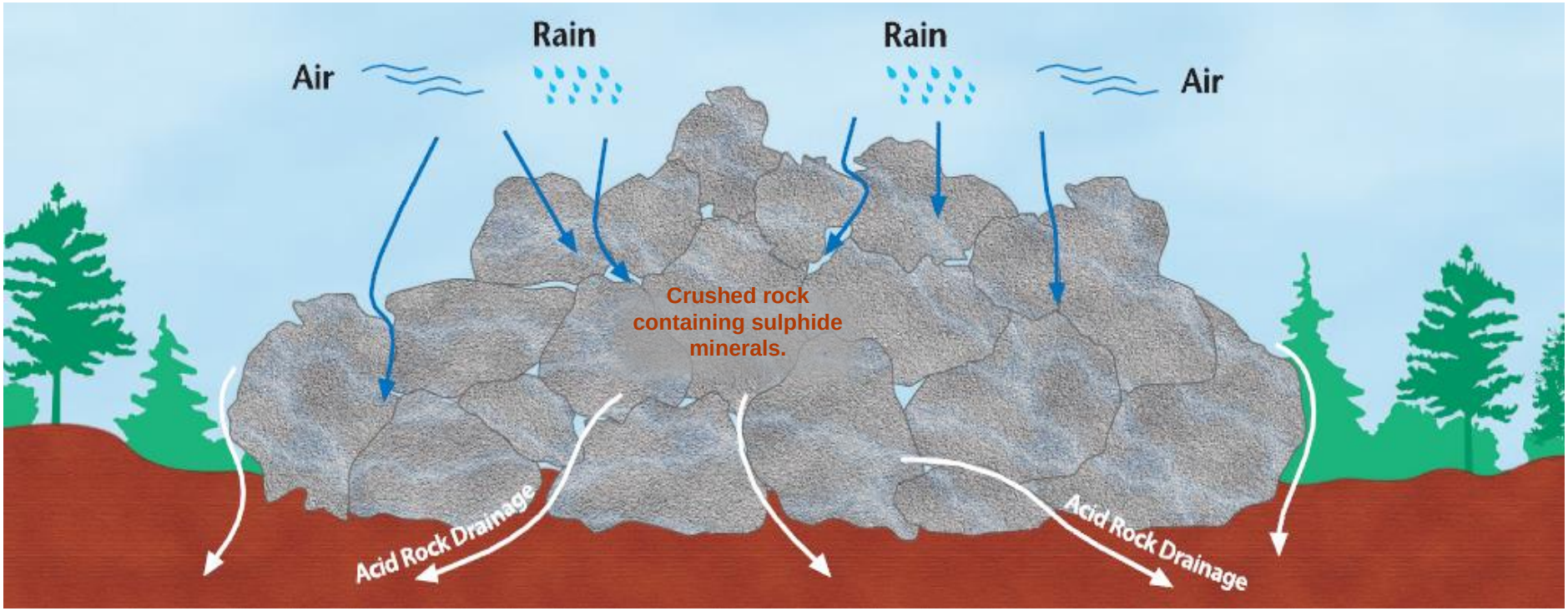

Key Mining Terms

Ore - rock containing sufficient quantities of minerals that make it valuable for mining

Milling - the process used to separate metals from ore

Waste Rock - rock of little economic value that must be removed to access the ore

Tailings - waste material left after metals have been removed from ore by milling

Diversion - an artificial channel that changes the natural course of a creek or stream

Pit - a large hole created when ore and waste rock is removed from the ground

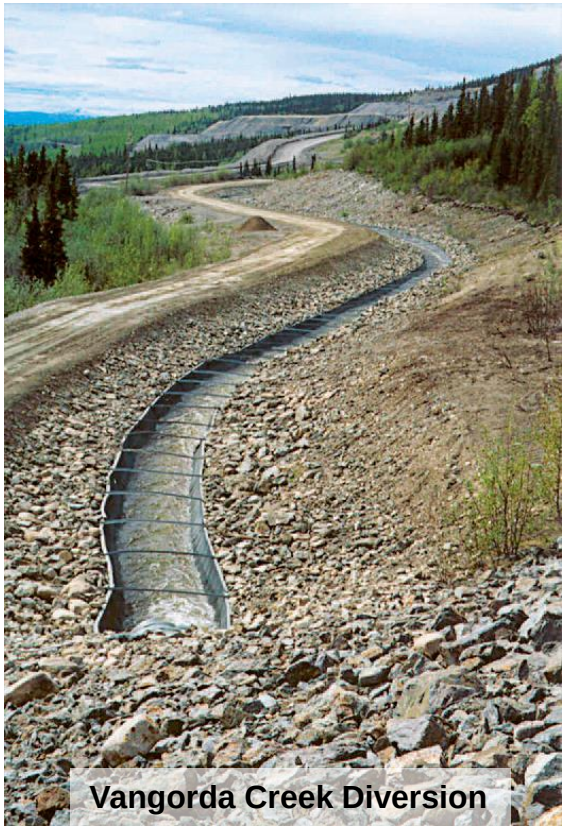

Vangorda Creek Diversion

Floatation Cells used in Milling

Waste Rock at the Faro Mine

Faro Mine Remediation Project:
Overarching Closure Objectives

Final closure and remediation plan Objectives:

1. Protect human health & safety
2. Protect, and to the extent practicable, restore the environment including land, air, water, fish and wildlife
3. Return the mine site to an acceptable state of use that reflects pre-mining land use where practicable
4. Maximize local and Yukon socio-economic benefits
5. Manage long-term site risk in a cost effective manner

Remediation and Closure

The recommended remediation (closure) plan is based on a **stabilize-in-place** approach

The preferred option emphasizes the need to stabilize contaminants, rather than remove them from the FMC.

Key features of the final remediation plan include

- Re-sloping waste rock
- Installing engineered soil covers over tailings and waste rock

- Installing state-of-the-art water collection and treatment systems. Water treatment at the Faro Mine Complex relies on lime precipitation technology.
- Upgrading the hydraulic capacity of dam spillways and creek diversions to pass large-scale flood events without failing the structures and potentially releasing mine waste and mine-impacted water to the environment

Water Treatment

Water management is the most important site operations activity at the FMC. Water management operations include operating, maintaining, repairing, and monitoring the following water management systems and facilities at the FMC:

- Fresh water conveyance systems
- Contaminated water collection, conveyance, and storage systems
- Interim Water Treatment System and Vangorda Water Treatment Plant
- Sludge management facilities

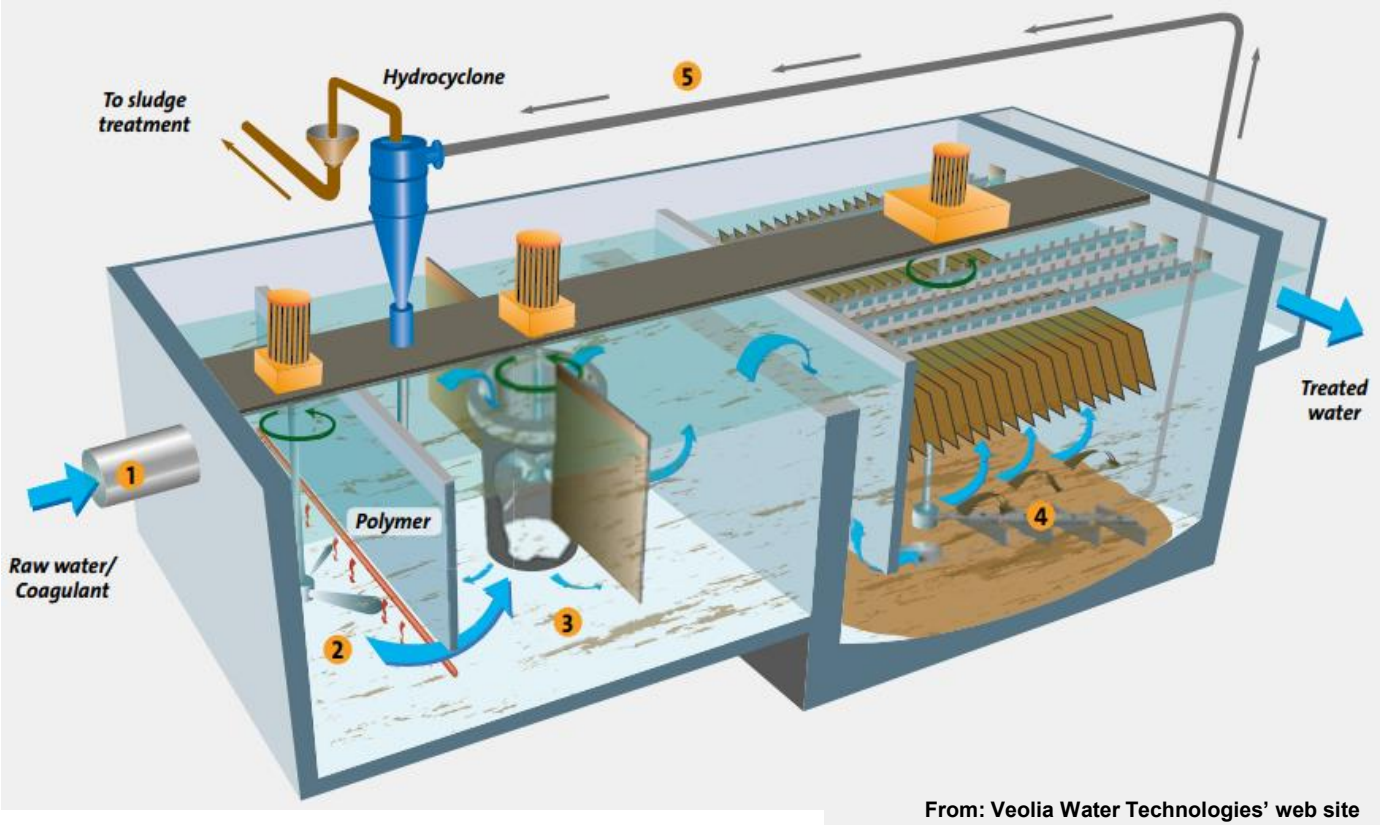

From: Veolia Water Technologies' web site

Illustration of treatment process used in the Interim Water Treatment System, commissioned in 2014

The Interim Water Treatment System (IWTS) is a modular lime-neutralization system. Slaked lime is used to raise the pH, and precipitate out metals. Zinc is the primary metal of concern at Faro.

Influent is split between two independent treatment trains, each with a treatment capacity of 189 L/s.

Effluent from the IWTS is discharged either directly to Rose Creek, or to a polishing pond for clarification.

Covers

Maintenance work on the GSC cover, 2011

A cover is a common measure to close a mine waste facility. The objective of a cover is to reduce the contact between contaminating materials and the environment. In the Faro Mine Complex, covers can be used to promote chemical stabilization of acid-generating materials. Covers are designed to minimize water infiltration and may limit exposure of wastes to oxygen.

During mining of the Grum Pit, sulphidic waste rock was preferentially placed in an area of the waste rock dump to form the Grum Sulphide Cell (GSC).

In 2010, a very low infiltration cover was installed over the GSC which consisted of a plastic liner overlain by 1 m of till. It has an area of 28 ha, and its main objective is to reduce infiltration to 0.5% of mean annual precipitation.

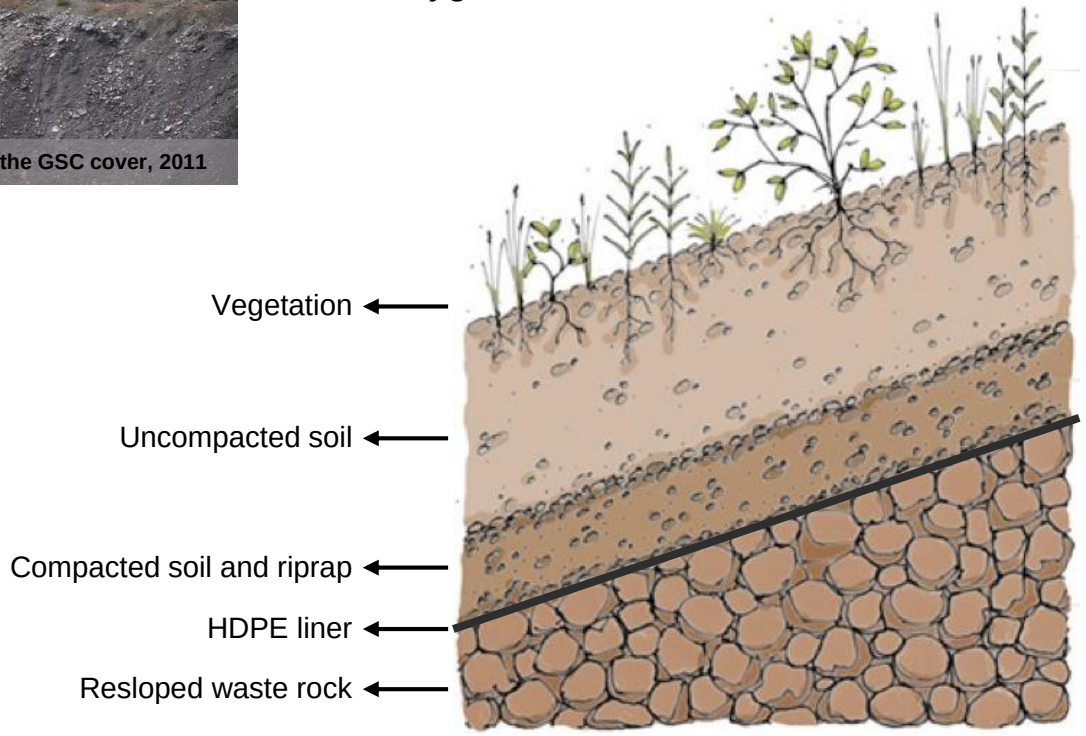

Faro Mine Complex: Site Inventory

Faro Mine Area

Vangorda Plateau

Components

70 million tonnes tailings
4 dams
1 open pit – Faro Pit
2 stream diversions
260 million tonnes waste rock

Components

No tailings
2 open pits: Vangorda & Grum
1 stream diversion
44 million tonnes waste rock

Faro Mine Complex Landmarks Map

Mining for lead and zinc at the Faro Mine began in 1969 and lasted for almost 30 years. During its operation, the mine processed between 5,000 and 9,300 tonnes of ore per day. In 1998, the owner, Anvil Range Mining Corporation, went into receivership and stopped all mining operations. The Faro Mine site is 25 km² or 2,500 hectares in size. There is a total of 70 million tonnes of tailings and a total of 386 million tonnes of waste rock on the site.

Faro Mine Remediation Project
Projet d'assainissement de la mine Faro

LEGEND

Creeks

Diversions
Channel that diverts clean water around the site.

0 0.5 1 2 KM

www.faromine.ca | info@faromine.ca

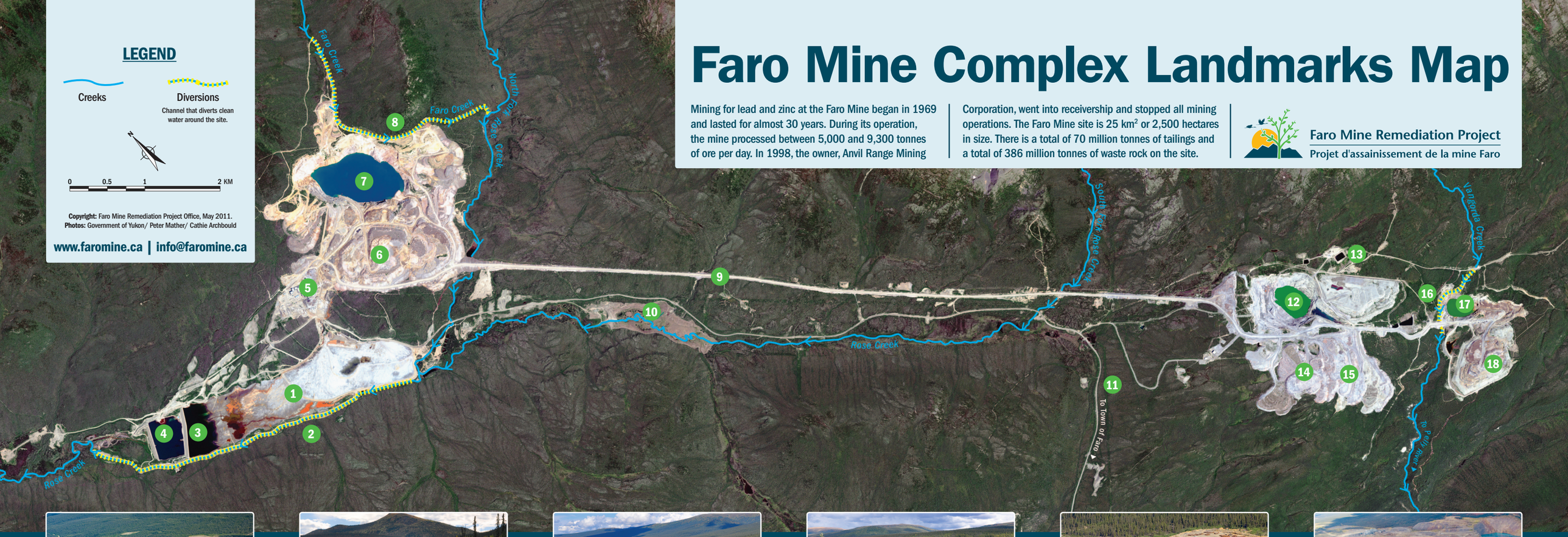

1. Rose Creek Tailings Area

2. Rose Creek Diversion

3. Intermediate Pond & Dam

4. Cross Valley Pond & Dam

5. Mill Area – Faro Water Treatment Plant

6. Faro Waste Rock

7. Faro Pit

8. Faro Creek Diversion

9. Haul Road

10. Fresh Water Supply Dam & Reservoir

11. Access Road

12. Grum Pit

13. Vangorda Water Treatment Plant

14. Grum Waste Rock

15. Grum Sulphide Cell Cover Project

16. Vangorda Creek Diversion

17. Vangorda Pit

18. Vangorda Waste Rock

Rose Creek Tailings Area

1. **Rose Creek Tailings Area** (RCTA) covers an area of over 200 hectares in the original valley of Rose Creek, just downstream of the confluence of the North Fork Rose Creek and South Fork Rose Creek. The RCTA is composed of four dams, containing 28.6 million m^3 (about 55 million tonnes) of acid-generating tailings and one diversion.
2. **Rose Creek Diversion** (RCD) is a 5 km long channel that diverts Rose Creek around the tailings storage area.
3. **Intermediate Pond and Dam** (IP) is a zoned earthfill embankment with a sloping upstream low-permeability core and a downstream shell. It retains mine-impacted water and tailings. It is the highest-risk geotechnical structure at the FMC.
4. **Cross Valley Pond** (CVP) is body of water held by a zoned dam with low permeability core and filters, it is used as a polishing pond for water treatment plant effluent.

Looking East; CVP (closer), IP (farther), and RCD (right). Located within RCTA.

Faro Mine Area

5. **Interim Water Treatment System** seasonally treats Faro Pit and Intermediate Pond water using a modular lime-neutralization system tied to a Veolia Water Systems Actiflo clarification system.

6. **Faro Waste Rock** Dumps are composed of waste rock deposited in a series of dumps surrounding the Faro Pit. There are approximately 260 million tonnes of waste rock in the Faro WRDs, covering an area of approximately 335 hectares. There are more than 30 separate dumps, with varying levels of mineralization. None of the dumps are considered completely benign.

7. **Faro Pit** is approximately 1,675 m long, 975 m wide, and 330 m deep and surrounded by piles of waste rock.

8. **Faro Creek Diversion** conveys Faro Creek along the northeast side of the Faro Pit and into North Fork Rose Creek. Faro Creek collects natural flows from a catchment north of the Faro Pit. The Creek originally flowed across the footprint of the Faro Pit and into Rose Creek via a channel located in the area now occupied by the Emergency Tailings Area.

Aerial photo (looking North) Faro Pit and Waste Rock, and Mill Area on the bottom left

Roads and Fresh Water

9 **Haul Road** is an approximate 10 km long road made of waste rock to connect the Faro Mine Area and the Vangorda Plateau. It was used to haul ore from the Vangorda Plateau to the mill for processing.

10 **Fresh Water Supply Dam and Reservoir** located on the South Fork Rose Creek provided water to the mill for processing during the low-flow winter periods. The dam was breached in 2004 to reduce the hydraulic risk to the RCTA downstream.

11 **Access Road** is a public highway that provides access to site from the Town of Faro.

Aerial photo (Looking West) Haul Road, Access Road, and breached Fresh Water Supply Dam (form left to right)

Vangorda Plateau

12 **Grum Pit** is approximately 1,000 m in length (north to south), and 625 m wide (west to east). It is located near a drainage divide, and its catchment area is approximately 1.5 km2.

13 **Vangorda Treatment Plant** was constructed to treat water from Vangorda Pit during mining operations. It now treats water from the Vangorda and Grum Pits before being released into Vangorda Creek.

14 **Grum Waste Rock Dump** contains about 28 million tonnes of waste that covers about 148 hectares. The south-central portion of the Grum WRD contains sulphide-dominant waste rock

Aerial photo (looking SW) We can see the Vangorda Pit and the Grum Waste Rock Dumps

15 **Grum Sulphide Cell Cover** is a 28 hectare, low-infiltration dry cover and associated water management system over highly-sulphidic part of Grum WRD.

16 **Vangorda Creek Diversion** conveys the Vangorda Creek around the Vangorda Pit.

17 **Vangorda Pit** is approximately 1150 m long, 350 m wide, and 150 m deep.

18 **Vangorda Waste Rock** is composed of over 16 million tonnes of waste rock surrounding the Vangorda Pit

Faro Mine Remediation Project

Projet d'assainissement de la mine Faro

Yukon Government

Canada